

Artificial intelligence assisted technoeconomic optimization scenarios of hybrid energy systems for water management of an isolated community

Rasikh Tariq^{*}, A.J. Cetina-Quñones, V. Cardoso-Fernández, Hernández-López Daniela-Abigail, M. A. Escalante Soberanis^{*}, A. Bassam, M. Vega De Lille

Unidad de Posgrado de la Facultad de Ingeniería, Universidad Autónoma de Yucatán, Av. Industrias No Contaminantes por Anillo Periférico Norte, Apdo. Postal 150, Cordemex, Mérida, Yucatán, Mexico

ARTICLE INFO

Keywords:

Water-energy nexus
Hybrid renewable energy systems
Potable water filtration
Wastewater treatment
Artificial intelligence
Digital twin
Optimization
Sensitivity analysis

ABSTRACT

Water is an essential resource demanded worldwide and it is quite debatable owing to the economic, political, and energy characteristics of any region. Off-grid water filtration plants are an alternative for communities where transportation of freshwater becomes a real challenge due to a lack of infrastructure for the water potabilization processes. For such potable water filtration plants, hybrid renewable energy systems (HRES) can be a viable solution to meet their energy demand meanwhile providing a sustainable water solution.

The main contribution of this work is the unique methodology, which starts with a sizing procedure of various hybrid energy systems using a commercial software “Hybrid Optimization of Multiple Energy Resources (HOMER)” and spreadsheet algorithms, followed by a “Non-dominating Sorting Genetic Algorithm II (NSGA-II)” based multi-objective optimization. Single-objective optimization scenarios contain photovoltaic installation capacity, wind turbines, diesel generators, and battery energy storage systems including Pb-acid (Lead-acid), Li-ion (Lithium-ion), and AGM (Absorbent Glass Mat) technologies as design variables to maximize the cost of electricity or net-present-cost. Multiobjective optimization also involved environmental (CO₂ emissions i.e. carbon dioxide emissions) and water cost indices as an additional packet to single-objective optimization scenarios. Afterward, a multicriteria decision-making tool using “The Order of Preference by Similarity to Ideal Solution (TOPSIS)” is applied on the Pareto front to attain the final optimization results. The analysis is further explored in depth by generating digital twins (surrogate or meta model) of HRES data using artificial intelligence techniques (artificial neural network and group-method-of-data-handling). Furthermore, calculus and statistical sensitivity analysis assist in the identification of the significant variables in the design procedure. In summary, the technical contribution of this work can be divided into two sections. The first one is the design of a hybrid energy system for the water management of an isolated community of the indigenous Mayan region of Yucatan, Mexico, which has never been considered before. Secondly, the technical contribution is related to the usage of environmental emissions as an objective function, which is not considered in the traditional design of hybrid energy systems by the software HOMER. Environmental emission as an objective function is not considered while designing a hybrid energy system in commercial softwares like HOMER, in fact, HOMER provides a list of environmental impacts but it is a secondary outcome as a result of technoeconomic optimization.

Analysis of results between HOMER pro and spreadsheet has shown conformity, reporting that the optimal case consists of a photovoltaic system, diesel generator, and Li-ion technology of battery storage with capacities of ~17 kW, ~5kW, and 44–48 kWh, respectively, corresponding to a net present cost ranging from 70,000 United States Dollars (USD) to 79,000 USD and a cost of electricity ranging from 0.205 to 0.229 USD/kWh. The achievements obtained with multiobjective optimization indicate that the cost of electricity and net present cost can be further reduced by 0.86 % and 0.73 %, respectively, at a decrement of only 0.4% of the renewable fraction as compared to the single objective optimization scenario. It is concluded that multiobjective optimization provides an add-in feature to HOMER by using environmental emissions as an objective function.

The design procedure and adapted methodology can be useful to promote sustainable development in the statewide context and can provide a scientific justification to national energy policymakers.

^{*} Corresponding authors.

E-mail addresses: rasikhtariq@gmail.com, rasikhtariq@alumnos.uady.mx (R. Tariq), mauricio.escalante@correo.uady.mx (M.A.E. Soberanis).

URL: <https://sites.google.com/view/rasikhtariq> (R. Tariq).

Introduction

Water is an essential resource [1], and in recent decades it has become scarce in some parts of the world [2]. The proportion of fresh water on the earth's surface is only 2.5 % but only 1 % is accessible for use [3]. Moreover, there is a growing water demand [4], and existing freshwater resources are not sufficient to meet human needs [5]. Coupled with this, the effects of climate change, the increase of pollution, and anthropogenic activities around the world have caused a decrease in water quality, which represents a big global problem, especially in marginalized communities with low quality of life [6]. Water quality in the water bodies is greatly dependent on physical, chemical, and biological parameters which must be evaluated before deciding the specific usage of water. Conventional water treatment plants ensure the necessary quality of water either for domestic or for drinking use [7]. However, they involve different processes such as filtration, chlorination, coagulation-flocculation, sedimentation, among others, which entail great energy consumption. Moreover, there are other costs such as transportation and distribution which limit its benefits to regions [8] that are situated away from the treatment plant [9]. For instance, in Mexico, the amount of energy required by a potable water treatment plant from the ground or surface is between 0.1 and 4.5 kWh/m³ [10]. This energy is obtained by the burning of fossil fuels, and consequently, the problem of environmental pollution and climate change persists. Therefore, renewable energy sources have emerged as an appealing alternative to conventional power generated from fossil fuels [11,12]. This has led to increasingly significant levels of distributed renewable energy generation being installed on existing distribution circuits. This brings the research to address the water-energy nexus in which no compromise should be made to utilize green energy resources for the potable water treatment plant.

There are different types of conventional and non-conventional energy sources used to generate electricity. Solar [13] and wind energy [14] systems are some of the most prominent sources of energy. The utilization of solar and wind energy systems has become increasingly popular due to their modular and environment-friendly nature [15–18]. The combination of solar and wind energy resources [19] has exhibited significant effectiveness in the previous two decades because of their standalone interactive utility. Nevertheless, due to the intermittent nature of solar and wind energy, the system based on either solar or wind energy alone is found unreliable. A system that is based on renewable resources but at the same time reliable is necessary and a solar-wind hybrid system with battery storage and a small diesel generator as a backup can meet this requirement. These systems may be utilized in grid-connected mode, isolated [20] from the grid and special aims, and are called Hybrid Renewable Energy System (HRES) [21]. There are several types of hybrid energy systems [22] such as wind-solar hybrid, solar-diesel, wind-hydro, and wind-diesel, which are among the present in production plants. The design and sizing of a system and the choice of energy resources depend on several considerations. It includes the type of storage system which is important for both on-grid and off-grid systems. The motivation to design and size a hybrid system is the following: reduction in the peak load (load shaving), provide energy security to the user application and minimize the effects of uncertainty related to renewable generation systems [23]. The strategic combination that minimizes the cost and maximizes the energy profit from a hybrid system can be attainable through an optimization study. For these reasons, it is important to locate the optimal operation in any energy system [24] with a requirement that a system must provide a consistent energy meeting the demand [25]. The factors affecting the choice of hybrid power technology can also tell us why people use hybrids and some of the advantages.

The usage of the techniques of machine learning has benefited and extended the research circle nearly in every area. Ahmed et al. [26] have applied machine learning in different types of networks and networking technologies to meet the requirements of future communicating devices

and services since the growing network density and unprecedented increase in network traffic require intelligent network operations. Sodhro et al. [27] provided a comparative analysis of various tools and applications in terms of energy efficiency with objective to minimize the energy consumption of software and hardware components. Sodhro et al. [28] also proposed the need for self-adaptive artificial intelligence-based strategies to effectively cluster, examine, and interpret the entire entities in the system. Memon et al. [29] provided an introduction to various key concepts of Wireless Local Area Network (WLAN) that are necessary to design, model, and develop a framework while also discussing Quality of Service for IEEE 802.11 WLAN and Medium Access Control protocols for supporting industrial emergency traffic over the network.

During the last years, many studies have been conducted in the area of HRES that includes different optimization techniques using machine learning in these applications. For instance, Sreeraj et al. [30] proposed a method that is based on the design space approach and can be used to determine the conditions for which hybridization of the system is cost-effective. The proposed method was implemented to design an isolated power system for an Indian village (Sukhalai, Hoshangabad district, Madhya Pradesh) utilizing the wind-solar photovoltaic system. It is reported that the cost of energy from a photovoltaic/battery (PV/battery) system was 0.38 USD/kWh (United States Dollar) and the same for the wind-battery system was 0.24 USD/kWh. The wind power generating system is a cheap source of electric power as compared to solar PV, but the variability of the power available from the wind is greater than photovoltaic solar energy [31]. Hence, if the reliability requirement is low, the wind battery system is cost-effective. Dursun et al. [32] developed a computational model that allows calculating the energy supplied by a stand-alone renewable hybrid power system that can be used in an electrolyzer for the production of hydrogen. The results of the proposed model are calculated and compared with experimental data. According to the obtained results, the annual hydrogen production is 34.3 kg whereas the differences between the real data and model data are quantified with Mean Square Error (MSE) with a value of 8.28e-7. Rohani et al. [33] designed a hybrid renewable energy system for the remote area in Ras Musherib located in the western region of Abu Dhabi. The hybrid system, which consisted of a photovoltaic (PV) array, wind turbines, batteries, and diesel generators, was designed to meet three known electric loads, 500 kW, 1 MW, and 5 MW to be able to fulfill the primary load for 250, 500, and 2500 household, respectively. The obtained results indicated that the hybrid system with 15 % of photovoltaic and 30 % of wind turbine capacity was found to be the optimal system for 500 kW average load with an initial cost of 4,040,000 USD and total net present cost of 14,504,952 USD over 25 years. The reduction in CO₂ emission achieved in this study for the 500 kW optimal hybrid system was 37 % as compared to the conventional diesel generator case.

Recently, Forough et al. [34] presented a methodology for energy management systems based on the multi-objective receding horizon optimization to find the optimal scheduling of HRES. The proposed hybrid system was experimentally installed in an educational building that comprises PV panels, wind turbine, battery bank, and diesel generator as the backup system. The results have shown that using a longer time frame (from 6 h to 24 h), the total share of renewable energy in supplying weekly demand can be improved up to 18.7 %. Hence, the proposed methodology can manage a system to make better use of resources resulting in improved system scheduling. Harajli et al. [35] presented a study of a hybrid solar PV/diesel system to assess the energetic, environmental, financial, and economic performances of a hybridized solar photovoltaic energy using first-hand data and information collected from the Palestinian, Lebanese, and Iraqi commercial and/or industrial sectors. Results have shown that hybrid PV/diesel systems have largely beneficial energy, environmental, and economic performances in all three countries, whereas their financial performance is also positive for Palestine and Lebanon.

Several recent studies have simulated the HRES using commercial

software and comparing the results with another method. Generally, most of these methods are computer programs. One example was presented by Eltamaly et al. [36], where the authors proposed a new methodology that uses the following input data: hourly wind speed, hourly radiation, and hourly load power with many different types of wind turbines and PV module types, which was used to optimize a PV/wind/battery energy system for ten locations in Saudi Arabia through a computer program which was compared with “Hybrid Optimization of Multiple Energy Resources (HOMER)”. The obtained results revealed that the cost per kWh of HRES was found between 0.3 and 11.8 cents/kWh and that obtained by HOMER between 10.6 and 12.8 cents/kWh, which indicated that the program developed was ideal for the optimization of hybrid systems and the cost range is within a reasonable margin for HRES investment by the private and government sectors. One year later, Eltamaly et al. [37] presented a design and simulation study of a wind system for five sites in Saudi Arabia through a computer program developed using Visual Fortran which was verified through an Excel spreadsheet. The obtained results indicated that the best site was Dhahran with a cost of ~5.84 cents/kWh using a KMW-ERNO turbine, while the worst site was Riyadh with a minimum kWh cost of ~12.81 cents/kWh using a GE (General Electric) Energy 2 turbine. That same year, Eltamaly et al. [38] developed a computer simulation program to design and optimize a self-contained battery/wind/PV hybrid power system for the city of Dhahran, Saudi Arabia. The main objective of this study was to determine the optimal size of each component of the energy system that would allow obtaining the lowest cost of kWh, which was compared with HOMER. The results revealed that the initial costs of the system, replacement, operation, and maintenance and the salvage price obtained with HOMER were \$46,780,000, \$20,161,322, \$18,644,542, and \$-6,920,542, respectively. The developed program by the authors were \$49,126,780, \$18,089,010, \$8,809,040 and \$-2,011,168 respectively. Therefore, the computer program is able to report reliable predictions and it is a useful tool for sizing and optimizing HRES.

Suresh et al. [39] presented a modeling and optimization study of an off-grid HRES where the main objective was to reduce the Total System Net Present Cost (TNPC), Cost of Energy (COE), unmet load, and CO₂ emissions using a Genetic Algorithm (GA) and HOMER Pro software for three un-electrified village hamlets in Chamarajanagar district, Karnataka state (India). The results of the two methods were compared with four combinations (biogas-biomass/solar/wind/fuel cell with battery) of hybrid renewable energy systems. The results indicated that compared with HOMER, GA was found to be the optimal solution supplying energy with 0 % unmet load providing a cost of energy of 0.163 USD/kWh which is more cost-effective than HOMER. Mokhtara et al. [40] presented a novel approach by integrating demand-supply management with particle swarm optimization and applying it to optimally designed off-grid hybrid PV/diesel/battery system for the electrification of residential buildings in an arid environment, using a typical dwelling in Adrar, Algeria, as a case study. The proposed HRES was first modeled by an in-house MATLAB code and then validated with the HOMER software. Moreover, techno-economic analyses including sensitivity study were carried out considering different battery technologies. The results have shown that the energy demand and total net present cost (TNPC) were reduced by 7 % and 18 % as compared to the case of using solely supply-side management. Also, it was found that PV/Li-ion represented the best configuration, with TNPC of 23,427 USD and Cost of Electricity (COE) of 0.23 USD/kWh.

In the context of the problem formulation, some hybrid technologies can provide a completely different approach to water treatment, especially for remote communities, where the cost of power transmission lines is expensive. Therefore, the implementation of HRES is highly recommended to ensure cost-effective, reliable power delivery, and consequently, potable water [41]. The existing literature reports a versatility coupling case studies with a considerable depth of analysis. However, the technical feasibility of a hybrid energy system should be evaluated further in the case of water filtration plants to address the

water-energy nexus [42]. The feasibility of such hybrid energy systems is extremely practical for isolated indigenous communities, like the one presented here as a case study (indigenous community of San Jose Tipech, Yucatan). Another gap identified in the literature is that the researchers have not used environmental emissions as an objective function to design a hybrid energy system especially for the water management of remote communities. Some authors have provided information about environmental emissions like the Ramesh et al. [43], Soberanis et al. [44], Sarker et al. [45], Shezan et al. [46], and Upadhyay et al. [47]. However, they have not used those emissions for the initial design. Moreover, the environmental emissions are presented merely as an outcome of the primary design. Thus, with this background, it is important to contribute further in this area by using environmental features of a hybrid energy system for the initial design of water filtration plants for remote communities

This is also aligned with the sustainable development goal no. 10, reduced inequality, of the United Nations. This research also addresses other sustainable development goals like 7, 8, 9, 11, 12, and 13 of the United Nations. On the other hand, there is a country-wise sustainable development goal to align with the goals of the United Nations. In this case, the national sustainable development goals of Mexico are also addressed which are a part of the national agenda 2030 [48]. Furthermore, the state of Yucatan has a statewide agenda too. Through the help of quantitative indicators, it is reported that the state of Yucatan is still struggling to meet the statewide goals, for example, the goal of clean water and sanitation, affordable and clean energy, and reduced inequality, are only attained by 37 %, 58 %, and 55 %, respectively [49]. This is a worrisome situation in which the state must put more effort and take diligent steps to address these issues. In this context, the current work can be a beacon to lift statewide sustainability indicators, contributing towards the national agenda 2030 with a projection towards the global sustainable development goals. Another justification of the work is related to the scientific development projects to address the national problems of Mexico specifically directly targeting (a) comprehensive water management, water security, and water rights, (b) mitigation and adaptation to climate change, (c) sustainable energy consumption, (d) development and use of clean renewable energies, and indirectly targeting, (a) fight poverty and food security.

Apart from addressing the sustainable development goals, technically, this study also bridges other gaps likesuch as the limitations of the usage of the software HOMER for hybrid energy systems. The optimization scenario considered in HOMER is based on a single objective optimization, considering linearly dependent net present cost and cost of electricity. However, in real-world conditions, the problem is multidimensional and requires extra indicators, specifically environmental emissions, contemplating the context of global warming challenges. Even though a renewable energy system does not have carbon dioxide emissions during the operation, it is marked with environmental emissions during the life cycle. Hence, even a renewable hybrid energy system should have a carbon dioxide accounting before implementation. In summary, the novelty of this work is to fill various gaps in the existing body of knowledge by addressing water-energy nexus through the integration of wastewater treatment and potable water filtration plant with the hybrid energy system. Moreover, it, addressing the statewide, national, and global sustainable development goals, and highlighting additional environmental add-in feature as an objective function for optimization purposes in the HOMER software.

Thus, the motivation of this work is to provide an integrated design of a hybrid energy system for the water management of an entire indigenous Mayan community located in the south-east of Mexico. The proposed design would help to mitigate various environmental, health, and social problems of the community and would significantly contribute to the sustainable development goals of the state. Another motivation of this work is to use environmental emissions as an objective function for the design of the hybrid energy system, which has a significant importance, considering the global environmental degradation

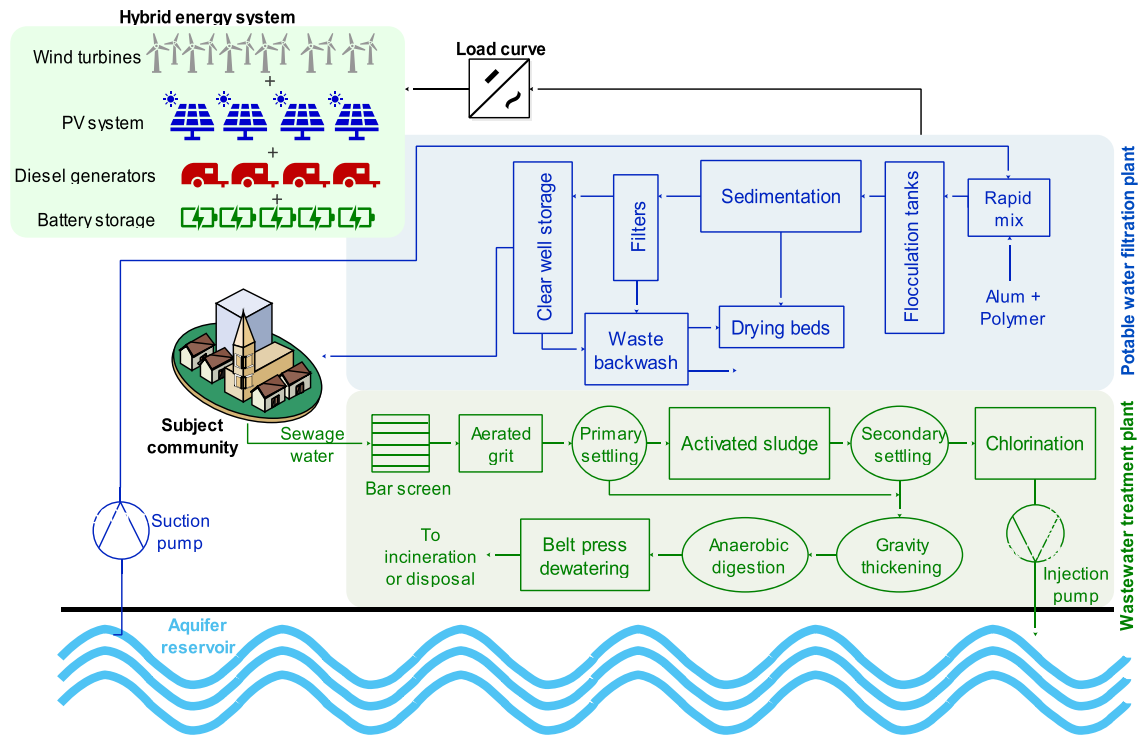


Fig. 1. Representation of the processes involved in the wastewater treatment plant and potable water filtration plant, considered for the sizing of the hybrid renewable energy systems.

problems.

The objectives of this research work is to evaluate the technical and economic indicators of different hybrid energy systems proposed to satisfy the energy demand of a suggested Wastewater Treatment Plant (WWTP) and Potable Water Filtration Plant (PWFP) for a remote community in the state of Yucatan. The authors used a spreadsheet whose results were compared with the software HOMER Pro, which led to a multiobjective analysis by using artificial intelligence techniques to find the optimal case and the different economic indicators that allowed to conclude the viability of the project. The model developed in the present work consists of a HOMER pro and developed spreadsheet techniques for the sizing of the HRES capable of supplying the energy demanded from the water treatment and filtration plants, followed by a multiobjective optimization process developed to further enhance the performance of both techniques. Furthermore, in relation to some previous studies reported in the literature [23,36–38], the methodology presented in this work consists of a complete study of an HRES with sizing, optimization scenarios, and sensitivity analysis. Also, there are few optimization studies reported in the literature where different scenarios are considered with different energy storage technologies. The developed spreadsheet allows to find the optimal combination of HRES that minimizes the COE and maximizes the Net Present Cost (NPC), and mainly contemplates three different storage technologies considering the initial costs and the lifetime of each one. Finally, it is also pertinent to mention that no research has targeted the usage of the hybrid energy system with a potable water filtration plant for an indigenous community of the Mayan region with the consideration of optimization scenarios built on HOMER, spreadsheet, and MATRIX Laboratory (MATLAB).

System description

In this section, the processes that take place for the water to be potable for its usage in the community as well as the ones involved in the wastewater treatment once the resource has been used are described. Fig. 1 presents the schematic diagram of the complete water cycle

highlighting each process involved in both water treatment plants, from its entry to the wastewater treatment plant to its final disposal in the community. The development of a similar model, where industrial wastewater and potable water treatment plant was analyzed, is reported by Gude [50]. Moreover, Fig. 1 illustrates that from the integration of both plants, a load curve is determined which describes the energy demand throughout the day. This load curve is used to size the hybrid renewable energy systems by different techniques.

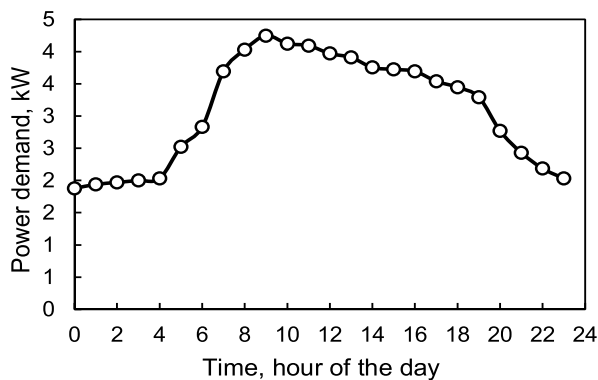
Wastewater treatment plant

The wastewater treatment process is divided generally into four steps. The first one consists of a preliminary treatment in which the objective is to remove the coarse solids and other large materials that are often found in raw wastewater. Preliminary treatment is carried out in the proposed treatment plant in the bar screen and aerated grit units. Subsequently, a primary treatment is carried out in the primary settling to reduce the suspended and floating solids in the wastewater by gravity action. Later, secondary treatment is carried out in the activated sludge unit, which is a biological process, since this consists of biological degradation of dissolved degradable organic matter and remaining suspended solids by microorganisms, reducing the organic loading in terms of COD (Chemical Oxygen Demand) and BOD (Biochemical Oxygen Demand), as well as nutrients like total nitrogen. It should be noted that during this treatment some nutrients or resources from the residual sludge can be recovered since they contain a considerable amount of nutrients, particularly phosphorus in the form of proteinaceous material [51]. Afterward, a secondary settling is used to remove the sludge (biological flocs) from the treated wastewater. Finally, in tertiary treatment, the purpose is to enhance the quality of the treated water to fulfill regulations for its discharge into the environment or reuse as a water source. This is done in the chlorination unit, which main purpose is the removal of pathogens. The final disposal of the water at the end of this process is in an aquifer reservoir, where it will be taken to be treated in the water purification plant described in the next section.

Table 1

Estimated energy consumption of the processes involved in the wastewater treatment plant and potable water filtration plant [50].

Loop of water plant	Process	Specific energy consumption (kWh/m ³)	Total energy consumption (kWh)
Wastewater treatment	Pumping	0.0317	6.791
	Screening	0.0081	1.743
	Aerated grit removal	0.0035	0.758
	Primary sedimentation	0.0041	0.877
	Activated sludge	0.1406	30.107
	Secondary sedimentation	0.0041	0.877
	Chlorination	0.0007	0.153
	Gravity thickening	0.0483	10.356
	Anaerobic digestion	0.0370	7.923
	Dewatering	0.0101	2.173
	Pumping	0.0317	6.791
	Alum + Polymer	0.0015	0.323
	Rapid mix	0.0081	1.743
Potable water filtration treatment	Flocculation tanks	0.0024	0.509
	Sedimentation	0.0023	0.498
	Drying beds	0.0011	0.226
	Waste backwash	0.0053	1.132
	Clear well storage	0.0053	1.132
	Total		74.11

**Fig. 2.** Hourly variation curve of the power demand for water treatment plants.

Additionally, large suspended solids and sludge coming from the primary and secondary settling are thickened (concentrated) in the gravity thickening and afterward stabilized in the anaerobic digestion unit. Finally, the stabilized sludge is passed through a belt press dewatering to remove excess water before disposal. The resulting sludge can be incinerated or used as a biosolid in agriculture.

Potable water filtration plant

The process begins by taking the water demanded by the community daily from the aquifer reservoir. First, it goes through a rapid mix which consists of identifying the solid suspended particles existing in the water and mixing them with the help of aluminum and polymers to form even bigger particles and making it easier for them to be extracted from the water. The flocculation tanks are the space where the water with the now visible suspended particles is received before entering the sedimentation process, where the heaviest components that remain in the fluid fall to the bottom of the container. The cleaned water goes to a final

filtration process to make sure that every solid particle has been eliminated and finally remains stored in a well until it's demanded by the subject community. The unwanted particles obtained in the last filtration process and some detected while in storage, are redirected to a waste backwash process where it reverses the flow of water lifting it and expelling the dirty water to a drying bed, or to the environment in case the pollution levels are low enough. Drying beds receive the particles obtained as a residue from the sedimentation process and along with the dirty water that comes out of the waste backwash, it forms a sludge that is dried by percolation and evaporation; the substance obtained from this process is often used as a biosolid in agriculture.

Methodology

Description of the study site

This research work evaluates energy and economic indicators of different hybrid energy systems proposed to satisfy the energy demand of a wastewater and potabilization plant suggested for the San José Tipceh community, Muna municipality (20.48 °N, 89.72 °W), Yucatán, México. This town has a population of 700 inhabitants [52], distributed in 148 homes, of which 100 % have electricity, 97.71 % have drinking water and 88.55 % have a toilet [53]. Moreover, the average daily water consumption per capita is estimated at 200 L [54]. The climate of this municipality is tropical savanna type, it has an average annual solar radiation of 388.84 W/m² during sunny hours, an ambient temperature, and wind speed of 25.18 °C and 5.21 m/s respectively.

Estimation of energy consumption of water treatment plants and power demand curve

To develop the sizing of the treatment plants, it is necessary to know the daily water consumption by the entire community. The parameters necessary to carry out this estimation are the number of inhabitants of the community, as well as for each house, the daily water consumption of a person, the peak and return factors. This parameter is estimated as [55]:

$$q = k_1 \cdot k_2 \cdot p \cdot w \cdot N / 86400 \quad (1)$$

where q is the water flow to be treated (L/s), k_1 is the peak factor (1.8 for simplified sewerage [56]), k_2 is the return factor (wastewater flow/water consumption), p is the average number of inhabitants per dwelling and N is the total number of dwellings in the community. The calculation of Eq. (1) resulted in a value of 2.479 L/s, which is equal to 214.2 m³/day of water to be treated. This result was used to estimate the energy consumption of the respective water plants that allow the sizing of the hybrid renewable energy system. Therefore, it is necessary to know the energy demand curve of the wastewater treatment plants and the water purification plant. In this study, a single energy consumption curve is considered, which corresponds to both water plants and consists of the average behavior of energy for each hour of the day. This allows to identify the periods with the highest consumption, as well as those in which the energy demanded from the plant is minimal.

Each water treatment plant has different processes. Table 1 lists each process involved in both water treatment plants illustrated in Fig. 1, as well as the unit energy consumption and the total consumption. These values were calculated considering the result obtained from Eq. (1) with the context of the wastewater and potable water filtration plant as presented in Fig. 1 [50].

Regarding the hourly power demand curve, a single curve is proposed for both plants, as mentioned above, since it is considered an ideal case of energy demand for a community. The behavior of the hourly power demand was estimated taking into account the variation of the hourly water flow, which are modeled through stochastic methods, considering comprehensive data from the Mexican National Water

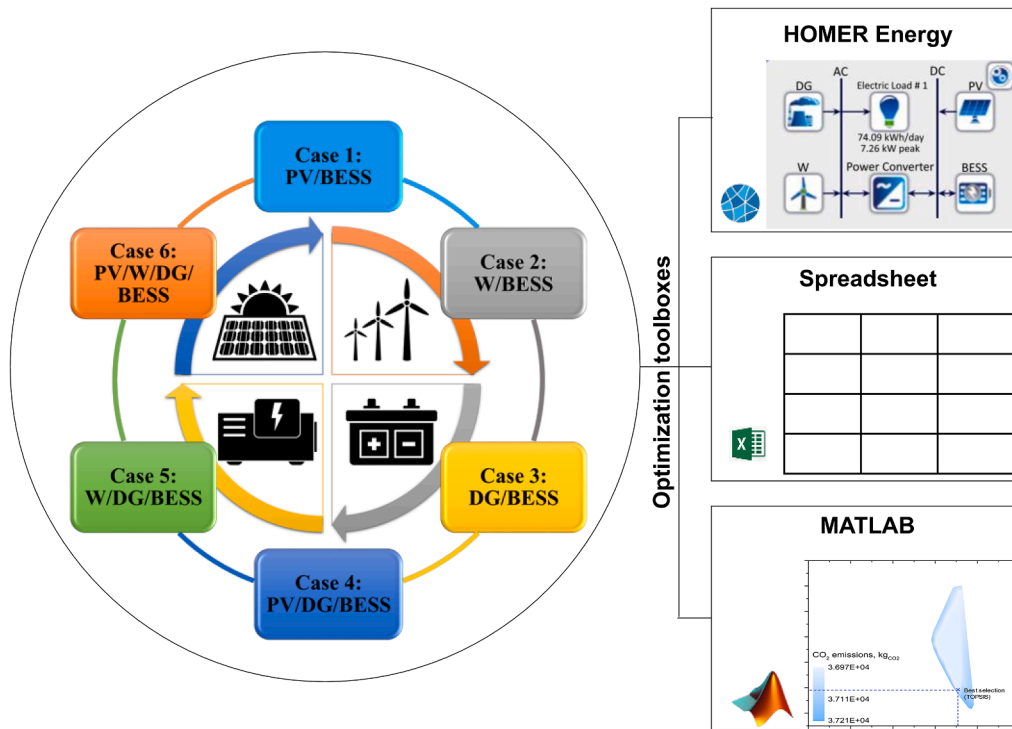


Fig. 3. Schematic diagram of the different cases proposed in this work.

Table 2
Technical specifications of photovoltaic modules [61].

Concept	Value
Brand and model	Sharp NU-JB395L
Maximum power	395 W
Nominal Operating Cell Temperature	45 °C
Temperature coefficient	0.353 %/°C

Commission (CONAGUA, by its acronym in Spanish) [57]. Fig. 2 illustrates the hourly power demand of the water treatment plants for the present case study. As seen in Fig. 2, the peak energy consumption occurs at 9:00 a.m., in which most people consume a greater amount of water since they take morning baths before leaving for work, and this trend continues throughout the afternoon, where housewives use a large amount of water for housework. However, during the night and in the early morning hours of the following day, water consumption is reduced, so that this behavior is reflected in the energy consumption of water treatment plants.

Sizing of the hybrid energy system

In this section, the sizing of the different combinations of the hybrid energy system consisting of a photovoltaic system (PV), a wind generation system (W), a battery energy storage system (BESS), and a diesel generator (DG) is proposed as a backup power system. For this purpose, different equations were considered that allow obtaining the average power and energy generated by each system throughout the year and estimating the number of elements by each system. For the case of a diesel generator, an HYUNDAI diesel generator model HHY5500 [58] with a nominal power of 5 kW was used, which has a fixed power, which does not depend on any renewable resource, but only on the volume of fuel to be used. Hence, the diesel generator is chosen based on the maximum power consumed by the study community to satisfy the maximum annual energy demand. The different proposed cases of the hybrid power system are illustrated in Fig. 3 along with the usage of

optimization toolboxes applied using HOMER energy, spreadsheet, and MATLAB.

Regarding the battery storage system, three different technologies were used: Pb-acid, Li-ion, and AGM, to obtain the most optimal technology from a technical and economic point of view. Finally, the photovoltaic and wind systems were modeled through different equations that allow estimating energy generation, considering different factors such as solar radiation, wind resource, ambient temperature, among others.

Photovoltaic solar system

The electrical energy production of a photovoltaic panel (PV) is given in terms of its temperature and the reference temperature for the design conditions [59].

$$P_{PV} = G_t \eta_{PV,ref} [1 - \beta(T_c - T_{ref})] \quad (2)$$

where G_t is the incident solar radiation on the PV module, $\eta_{PV,ref}$ is its efficiency under the reference temperature T_{ref} which is 20 °C, β is the temperature coefficient specified by the manufacturer and T_c is the temperature of the panel cell according to the NOCT criteria, which is calculated as follows [60]:

$$T_c = T_{amb} + \left(\frac{NOCT - 20}{800} \right) G_t \quad (3)$$

Here T_{amb} is the ambient temperature. The specifications of the photovoltaic modules proposed in this work are presented in Table 2.

The energy losses for the photovoltaic system and inverter were considered to be 3 % [62].

Wind generation system

To calculate the power generated by the wind turbine, the power curve from the datasheet of the wind generator to be implemented can be used so that this power is given as a function of the wind speed at the height of the wind turbine [63].

The proposed wind turbine, as well as its technical specifications, are detailed in Table 3.

Table 3
Wind turbine technical specifications [63].

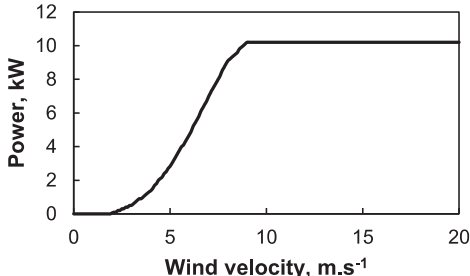
Concept	Value
Brand and model	Enair E200
Maximum power	10 kW
Diameter	9.8 m
Hub height	40 m
Power characteristic curve	

Table 4
Technical specifications of storage batteries [64].

	Technology		
	Pb-acid	Li-ion	AGM
Number of cycles (80% discharge)	1500	3500	2500
Allowable discharge depth	40 %	15 %	20 %
Energy losses (charge–discharge)	10 %	10 %	10 %
Lifetime	5 years	10 years	8 years

Table 5
Economic data used in this work.

System	Concept	Value
Photovoltaic	Capital cost	1,000 USD/kW [65]
	O & M	20 USD/kW [65]
Wind	Capital cost	5,000 USD/kW [65]
	O & M	30 USD/kW [65]
Power converter	Capital cost	1,000 USD/kW + 500 USD/kW additional [66]
Diesel generator	Unit cost	754 USD [58]
	O & M	0.025 USD/kWh [67]
	Fuel cost	2 USD/L [44]
Battery (Pb-acid)	Storage capacity	200 USD/kW [64]
Battery (Li-ion)		500 USD/kW [64]
Battery (AGM)		400 USD/kW [64]

Energy losses in the power converter are estimated to be 3% [62].

Battery energy storage system

The battery storage system comprises three different technologies: Pb-acid, Li-ion, and AGM. Each technology has different specifications regarding the number of charge–discharge cycles, energy losses, charge and discharge depth, and lifetime. These parameters are specified in Table 4.

The nominal capacity of each battery bank varies to find the optimal value that presents the lowest possible cost integrated with the hybrid renewable energy system. For the economic analysis, different costs were considered in each system, which is described in the following section.

Economic study of the hybrid energy system

This section describes the procedure used to calculate the economic indicators proposed in this work that allows decision-making of the system that presents the lowest net present cost and the lowest energy cost. To carry out the economic study, it is necessary to know certain

economic data of the hybrid system such as the capital cost of each system, the cost of the storage system capacity, operation and maintenance (O&M) costs, among others. These parameters are presented in Table 5.

To carry out the economic study to find the best combination of the system, two economic indicators were used: Net Present Cost (NPC) and Cost of Energy (COE). The NPC (USD) of a project is defined as the present value of all the costs of installation and operation of the system during the useful life of the project minus the present value of all the income obtained during the useful life of the project and is calculated by the Eq. (4) [33]:

$$NPC = \frac{C_{ann,tot}}{CRF(i, R_{proj})} \quad (4)$$

where $C_{ann,tot}$ is the total annuity and $CRF(i, R_{proj})$ is the capital recovery factor used to calculate the present value of an annuity, and it can be calculated using Eq. (5) [33]

$$CRF(i, R_{proj}) = \frac{[i(1+i)^n]}{[(1+i)^n - 1]} \quad (5)$$

where i represents the interest rate, of which 10 % per year was considered and n is the number of years, considering the 20-year duration for this project.

Finally, the COE (USD/kWh) is an indicator that represents the current cost to buy energy, so the objective is to minimize this value [68], which can be calculated as Eq. (6):

$$COE = \frac{NPC}{E_c} \quad (6)$$

where E_c is the total load of the community over 20 years.

Supplementary initial data

Details of some other initial data are given as follows:

1. Variable and hour-dependent elevation and declination angle are considered for the sizing of the photovoltaic system [69].
2. The efficiency used for the inverter is 97 % [70].
3. For the wind generation system, power obtained at different altitudes is analyzed through the use of wind shear [71].
4. In the case of the diesel generator, it is turned on and off following the recommendable percentages of minimum and maximum state of charge of the battery technology [64].
5. The utilized economical parameters are as follows: a minimum rate of return on investment of 10 %, annual increase on the costs of O&M of 5 % [72], annual inflation of 5 % [73] is considered.
6. Regarding the environmental parameters, both sizing techniques utilized the solar radiation, ambient temperature, and wind speed database which is obtained from NASA (National Aeronautics and Space Administration) Power Data Access [74].
7. Energy tariffs [75] and the cost of potable water [54] are taken from the Mexican electricity and water main suppliers, respectively.

Results and discussion of single-objective optimization using HOMER and spreadsheet

The sizing of the hybrid systems was carried out through the HOMER Pro software, as well as using a developed algorithm developed in an Excel spreadsheet. There are two optimization algorithms within the interface of HOMER Pro software. The original grid search algorithm simulates all the feasible configurations as defined by the search space. The other algorithm is related to a proprietary derivative-free algorithm that searches the least costly system and finally, the software displays the list of configurations sorted by the net present cost which is used for

Table 6
Results were obtained from the spreadsheet and HOMER for the three battery technologies.

Case	Technology	NPC (USD)		COE (USD/kWh)		PV capacity (kW)		W capacity (kW)		DG capacity (kW)		BESS capacity (kWh)		Power converter (kW)	
		Spreadsheet	HOMER	Spreadsheet	HOMER	Spreadsheet	HOMER	Spreadsheet	HOMER	Spreadsheet	HOMER	Spreadsheet	HOMER	Spreadsheet	HOMER
Case 1: PV/BESS	Pb-acid	98,264	82,703	0.286	0.240	25.7	19.9	-	-	-	-	85	87	5.3	7.4
	Li-ion	87,336	74,521	0.254	0.217	21.3	18.3	-	-	-	-	48	55	5.3	7.2
Case 2: W/BESS	AGM	92,029	74,976	0.268	0.218	23.7	19.9	-	-	-	-	54	55	5.3	7.3
	Pb-acid	259,027	230,298	0.754	0.670	-	-	30	30	-	-	130	124	5.3	7.3
Case 3: DG/BESS	Li-ion	248,275	236,589	0.722	0.667	-	-	30	30	-	-	80	88	5.3	7.3
	AGM	257,607	238,612	0.749	0.635	-	-	30	30	-	-	86	77	5.3	7.3
Case 4: PV/DG/BESS*	Pb-acid	248,123	238,903	0.722	0.695	-	-	-	-	5	5	6	6	-	-
	Li-ion	238,047	236,589	0.692	0.688	-	-	-	-	5	5	3	3	-	-
Case 5: W/DG/BESS	AGM	239,039	238,612	0.653	0.694	-	-	-	-	5	5	4	4	-	-
	Pb-acid	81,216	77,826	0.236	0.226	19.7	18.3	-	-	5	5	65	75	5.3	6.8
Case 6: PV/W/DG/ BESS	Li-ion	78,732	70,415	0.229	0.205	17.7	17.0	-	-	5	5	44	48	5.3	6.8
	AGM	84,271	71,207	0.245	0.207	19.7	18.1	-	-	5	5	45	49	5.3	6.5
Case 7: W/DG/BESS	Pb-acid	112,920	111,989	0.328	0.326	-	-	10	10	5	5	77	28	5.3	4.4
	Li-ion	102,862	101,359	0.299	0.295	-	-	10	10	5	5	36	34	5.3	4.9
Case 8: PV/W/DG/ BESS	AGM	101,885	100,294	0.296	0.294	-	-	10	10	5	5	25	35	5.3	5.1
	Pb-acid	116,693	111,244	0.339	0.323	12.2	12.5	10	10	5	5	57	62	5.3	9.1
Case 9: PV/W/DG/ BESS	Li-ion	114,229	110,940	0.332	0.323	12.2	12.5	10	10	5	5	38	44	5.3	9.1
	AGM	115,781	104,005	0.337	0.302	11.4	10.5	10	10	5	5	39	43	5.3	6.1

* The annual behavior of total load and total power output of the optimization configuration (case 4 with Li-ion battery) is displayed in Appendix A.

the comparison purposes of different system designs [67].

There is a dedicated algorithm which defines the operational behavior in various cases of the supplied loads by PV, diesel generators, wind turbines, and batteries. It also includes the usage of the charging and discharging cycles of the batteries. Halabi et al. [76] and Alsham-mari et al. [77] have described this energy management strategy in detail. The system operates in different modes according to the conditions of the surrounding atmosphere. During the normal and standard operating conditions when the sun is available, the control system gives the highest priority to the arrays of solar panels to supply the demand of the load. At this duration, the excess energy of the system is used to charge the battery until it reaches its maximum state of charge position. If there is a sufficient amount of solar radiation which generates enough photovoltaic electricity to meet the load and also charges the batteries to the maximum state of charge, then the excess energy is used by the dumped loads. In another case, when the solar panels can not provide sufficient electricity to handle the variation in the load, the batteries start operation and handle the load until reaching their minimum state of charge. If the renewable energy potential of some particular hours of the year is not sufficient enough to carry the supply load, and the batteries are also reaching their minimum state of charge, then the diesel generator is turned on and supplies the entire load. This control management system is sensitive to hourly calculations

Table 6 reports the comparison of the six cases illustrated in Fig. 3 with the three different battery technologies, contrasting the results of the spreadsheet and HOMER. Various technical parameters of each case are reported, as well as economic indicators. It is possible to observe that the results obtained from the spreadsheet are well correlated with the results obtained from HOMER. Considering the minimum values obtained by each technique used for sizing the hybrid systems, the best results regarding the cost of energy are obtained in the following order: case 4, case 1, case 5, case 6, case 3, and case 2.

There are different parameters hidden in each case, leading them to different COE scenarios. For instance, the cost of installation for 1 kW of wind turbines is much more expensive than for photovoltaic modules, with the hub being one of the most expensive parts of this technology. This is due to the three cases with wind turbines are the worst COE scenarios, just after the diesel generator with a battery storage system, which is affected considerably by the high cost of the fuel. Moreover, cases with photovoltaic modules resulted in two of the three best COE scenarios, since this renewable technology has been developing with success worldwide, making its cost of installation way lower than the one for wind turbines. The climatic conditions of the region are also a key point for analyzing the obtained results since the Yucatan peninsula is well known for its solar resource with solar daily radiation above the national average.

Furthermore, important features were discovered while comparing the results obtained between the spreadsheet and HOMER. From the results obtained with HOMER for case 1, the capacity proposed for the photovoltaic system is 21.3 kW for the Li-ion battery technology, while the capacity for the power converter is 7.2 kW, only 34 % of the total capacity of the photovoltaic system. From this percentage, it is possible to ensure that HOMER uses a charge controller since the power converter does not have the capacity enough to convert all the energy generated from the photovoltaic system, from DC (direct current) to AC (alternating current). Due to this observation, a charge controller was added to the calculations developed in the spreadsheet. This led to a decrease in the capacity of the power converter, as well as a modification in the COE regarding the cost of the charge controller.

Another difference discovered between the spreadsheet and HOMER was the batteries' limit level of charge. The only percentage that HOMER reports is the limit level of discharge, whereas, in the spreadsheet, both charge and discharge limit levels are modified according to the technology used. This led to reducing the number of batteries in the spreadsheet calculations regardless of the technology used for each case. Otherwise, analyzing the development that photovoltaic modules have

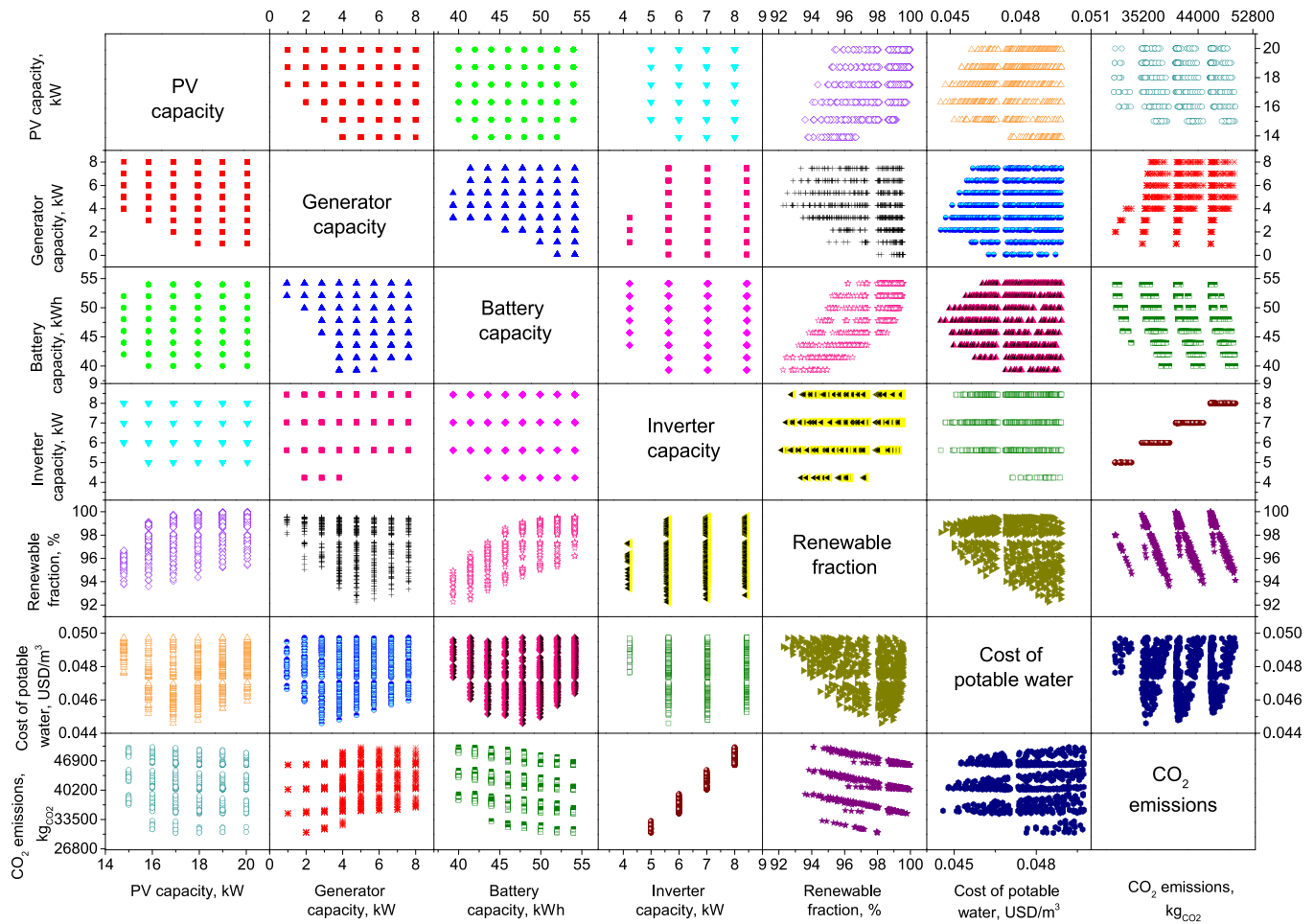


Fig. 4. Scatter matrix plot providing information on the generation of the numerical experiments for surrogate modeling.

had in the last 20 years, as well as results obtained from other authors on the sizing of hybrid systems, it is justified that a hybrid system integrated photovoltaic modules with a diesel generator and battery storage system is the optimal solution since wind turbines are still way too expensive for them to be used in a small demand project, comparing it with photovoltaic modules. The combination of wind turbines with diesel generators gives this renewable energy a chance to decrease its COE and have a better-looking scenario for future applications.

In general, it can be seen from Table 6 that the economic indicators obtained by the spreadsheet are higher than the ones presented by HOMER. This is due to the fact that the best scenarios calculated with the spreadsheet were obtained through a manual search, by changing unit by unit the nominal capacity of the elements that integrate each case. As for HOMER, it is software that calculates automatically the economic indicators taking into consideration the elements provided: photovoltaic modules, wind turbine, power converter, diesel generator, and energy storage systems. As a consequence, the computational time required from HOMER to present its results is much higher than the one associated with the spreadsheet.

Finally, from these results, it can be concluded that the best result obtained by these techniques was case 4 with Li-ion batteries technology since the NPC and the COE were minimized. These results were conducted to develop an optimization process to maximize the renewable fraction, minimize the cost of potable water, and reducing CO₂ emissions.

Sequential procedure of multi-objective optimization

Optimization involves a stepwise procedure that starts from the generation of a database, otherwise called 'numerical experiments', followed by the development of the digital twin, and finally, the actual optimization is accomplished.

Generation of numerical experiments

The first step in the development of a digital twin is correlated with the generation of a set of 'numerical experiments' which mimic a working database having all the required information of the input variables and the output indicators. In this case, such a database is generated using HOMER [78] having the following characteristics of the tuning parameters: (a) the PV capacity is varied from 15 kW to 20 kW, (b) the generator capacity is varied from 1 kW to 8 kW, (c) the battery storage capacity is varied from 40 kWh to 55 kWh, and (d) the inverter capacity is varied from 5 kW to 8 kW. The variation of this set of input variables is noted on the indicators like a renewable fraction, cost of potable water, and the CO₂ emissions which are depicted in Fig. 4. Fig. 4 also presents the sensitivity analysis of the input variables on the output variables. It can be noted that the renewable fraction increases stepwise with the increase in PV capacity and battery capacity, however, it increases with the decrease in CO₂ emissions. Also, the relationship between renewable fraction and the cost of potable water is not well defined. Therefore, it appears to be a multi-objective problem where it is desired to have high renewable energy penetration while maintaining a low cost of potable water [79].

Table 7

Selection of best architecture for the surrogate modeling of the performance indicators in the multi-objective optimization scenario.

Renewable fraction (%)							
Sample	Training algorithm	Number of hidden layers	R ²				Epoch
			Training	Validation	Testing	Total	
1	Levenberg–Marquardt algorithm ¹	1	0.82	0.82	0.77	0.81	16
2	Levenberg–Marquardt algorithm	4	0.92	0.86	0.84	0.90	29
3	Levenberg–Marquardt algorithm	6	0.92	0.92	0.92	0.92	32
4	Levenberg–Marquardt algorithm	8	0.94	0.94	0.95	0.94	16
5	Levenberg–Marquardt algorithm	10	0.94	0.94	0.95	0.94	17
6	Bayesian regularization algorithm ²	8	0.93	0.95	0.92	0.94	176
7	Scaled conjugate gradient algorithm ³	8	0.92	0.93	0.92	0.92	41

Cost of potable water (USD/m ³)							
Sample	Maximum number of input neurons ⁴	Input source ⁴	Maximum number of neurons ⁴	Polynomial power ⁴	Total SSE	Total MSE	Total R ²
1	2	0	1	2	0.000326	4.96E-07	0.689437
2	2	0	1	3	0.000325	4.96E-07	0.689649
3	2	0	2	2	0.000231	3.52E-07	0.779515
4	2	0	8	2	9.13E-05	1.39E-07	0.912947
5	3	0	5	3	7.56E-05	1.15E-07	0.927917
6	3	0	6	2	8.82E-05	1.34E-07	0.915908
7	3	1	5	2	3.97E-05	6.06E-08	0.962085
8	3	1	5	3	5.38E-06	8.20E-09	0.994867
9	3	1	6	2	4.98E-05	7.59E-08	0.952509
10	3	1	10	3	8.45E-06	1.29E-08	0.991942

CO ₂ emissions (kgCO ₂)							
Sample	Training algorithm	Number of hidden layers	R ²				Epoch
			Training	Validation	Testing	Total	
1	Levenberg–Marquardt algorithm	4	0.99	0.99	0.99	0.99	45
2	Levenberg–Marquardt algorithm	6	0.99	0.99	0.99	0.99	73
3	Levenberg–Marquardt algorithm	8	0.99	0.99	0.99	0.99	94
4	Bayesian regularization algorithm	8	0.99	0.99	0.99	0.99	145
5	Scaled conjugate gradient algorithm	8	0.99	0.99	0.99	0.99	104

¹ Levenberg–Marquardt algorithm typically required more memory but less time. Training automatically stops when generalization stops improving as indicated by an increase in the mean square error of the validation samples.

² Bayesian regularization algorithms typically require more time but can result in good generalization for difficult, small, or noisy datasets. Training stops according to adaptive weight minimization.

³ Scaled conjugate gradient algorithm typically required less memory. Training automatically stops when generalization stops improving as indicated by an increase in the mean square error of the validation samples.

Bold rows show the best architecture.

⁴ Referenced from the work [92].

The cost of potable water (USD/m³) and the CO₂ emissions (kgCO₂/kWh) are calculated using the following equations:

Development of a digital twin through the techniques of artificial intelligence

Digital twins (also called metamodels or surrogate models), which is a digital duplicate of a physical model, are gaining popularity in energy

$$\text{Cost of potable water} = \frac{\text{NPC}}{\text{Project life time (years)} \times \text{Hours in a day} \times \text{daily water demand}} \quad (7)$$

$$\text{CO}_2 \text{ emissions} = \sum_{i=1}^{\text{number of power sources}} (\text{CO}_2 \text{ emission factor} \times \text{Capacity of power source})_i \quad (8)$$

In Eq. (7), the project lifetime has 20 years, and the daily water demand is 214.2 m³/day (see section 3.2), yielding the units USD/m³ of the cost of potable water. In Eq. (8), the CO₂ emission factor of photovoltaic panels, batteries, generator, and inverter are 0.032 kgCO₂/kWh [80,81], 0.11 kgCO₂/kWh [82–84], 0.778 kgCO₂/kWh [81], and 0.641 kgCO₂/kWh [85–87], respectively.

systems [88,89] owing to their easiness of usage in the optimization process. The prime purpose of the generation of such a metamodel is correlated with complicated mathematical models and is associated with a high computational burden. Consequently, such physical models are not user-friendly for the multi-objective optimization process where the model is evaluated various times during the mutation, selection, and crossover operations to find the best fitness function. In such cases, a simplified digital twin can significantly reduce the optimization computational times because it just consists of a black box with a set of input variables and one or more output variables, whereas, the physical model consists of energy balances, control strategies, parameter calculations, and verification processes of assumptions. The digital twin is generated using the data-driven fitting techniques of artificial

intelligence including the application of artificial neural network (ANN), and group-method-of-data-handling (GMDH).

ANN consists of a feed-forward multilayered perceptron neural network which is applied for the metamodeling of renewable fraction and CO₂ emissions. For this process, the database is divided into three parts corresponding to training, validation, and testing sets making percentages of 70, 15, and 15, respectively. The training dataset trains the neural network for an appropriate fit, the validation assures that the training dataset does not overfit the database, and finally, the testing database is used to verify the regression fit. ANN consists of a particular architecture¹ in which the training algorithm and the number of hidden layers are the tuning parameters. An appropriate combination of these two tuning parameters must be evaluated for the development of the metamodel. MATLAB neural network toolbox is utilized for this method. It can be seen in Table 7 that the most suitable training algorithm for the renewable fraction is Levenberg–Marquardt having a neural network of 8 number of hidden layers corresponding to an R² (Coefficient of determination, see Appendix B) value of 0.94. Similarly, the most suitable training algorithm for CO₂ emissions is also Levenberg–Marquardt having a neural network of 6 number of hidden layers corresponding to an R² value of 0.99. The regression fit of the selected architectures of renewable fraction and CO₂ emissions are presented in Fig. 5(a) and Fig. 5(c). It can be noted from Fig. 5(a1 and c1) that datapoints follow the linear pattern between the target and the output variables having acceptable error performance indicators (RMSE(Root-Mean-Square-Error) = 0.460, SI(Scatter Index) = 0.46 %, MAPE(Mean Absolute Percentage Error) = 0.0029 for renewable fraction, and RMSE = 184.7, SI = 0.23 %, MAPE = 0.0035 for CO₂ emissions). It can also be noted from Fig. 5(a2 and c2) that there is no visible pattern in the error distribution that guarantees the independence and homoscedasticity of errors. Similarly, it can be noted from Fig. 5(a3 and c3) that the error distribution is also normal which guarantees satisfaction towards the neural regression model.

The cost of potable water is digitally modeled using the GMDH technique. It belongs to the family of polynomial neural network². However, this technique is a self-organizer that performs an automatic evaluation of the number of neurons, layers, and transfer function. This technique is only adapted for the digital twin generation of cost of potable water because ANN could not produce a satisfactory model owing to the manual evaluation of the training algorithm and the number of hidden layers. Nevertheless, GMDH comes up with other types of tuning parameters which are (a) the maximum number of input neurons, input source, the maximum number of neurons, and the polynomial power. It is implemented in MATLAB [90] using the algorithm published by Sohani et al. [91]. The dataset of the numerical experiments is only divided into two parts corresponding to the testing and training phases scoring 85 % and 15 %, respectively. Through a set of iterations, it can be noted from Table 7 that the most suitable architecture is sample no. 8 yielding an R² of 0.994. The regression fit which can be seen in Fig. 5(b1) shows the suitability of fit in which RMSE = 0.00013, SI = 0.23 %, and MAPE = 0.0019. Similarly, the test on the errors can be verified from Fig. 5(b2 and b3).

It is extremely vital to verify and validate the generation of the digital twins because the quality of the optimization process completely depends upon it. Therefore, extensive external validation of these digital twins is carried out which is attached in Appendix C. This gives sufficient confidence to the authors to claim the reliability of the digital twins and can be employed in the optimization process.

Problem formulation of multi-objective optimization

Multi-objective optimization is applicable in the situation where there is a trade-off (or conflict) between the objective functions. Therefore, the prime objective is to provide an upgrade to the baseline case conditions and the single objective optimization results. The formulation of the multi-objective optimization problem involves the presentation of the objective function, design variables, and the search space. It should be noted that the current problem is an unconstrained multiobjective optimization problem, and it is described as follows:

1. Objective functions for multiobjective optimization: In multiobjective optimization, it is desired to maximize the renewable fraction, and minimize the cost of potable water and CO₂ emissions. Mathematically, it can be written as:

$$\text{Min}(\text{obj}) = \begin{cases} \text{obj}_1 : -\text{Renewable fraction} \\ \text{obj}_2 : \text{Cost of potable water} \\ \text{obj}_3 : \text{CO}_2 \text{ emissions} \end{cases} \quad (9)$$

Note: The renewable fraction is multiplied by a negative one to accommodate the syntax of the optimization problem and the algorithm, therefore, the minimization of $\text{obj}_1 : -\text{Renewable fraction}$ yields its maximum value. obj refers to the objective function.

2. Design or tuning variables: The optimization is carried out based on the following design variables: PV capacity, generator capacity, inverter capacity, and battery capacity.

3. Search space for optimization: The optimization problem is constrained with a set of limits on the design variables which defines the search space or solution zone for the multiobjective algorithm. This space is expressed mathematically in the following equation:

$$\begin{aligned} 15 \text{ kW} &\leq \text{PV system} \leq 20 \text{ kW} \\ 1 \text{ kW} &\leq \text{Diesel generator} \leq 8 \text{ kW} \\ 40 \text{ kWh} &\leq \text{Batteries capacity} \leq 54 \text{ kWh} \end{aligned} \quad (10)$$

The constrained search space on the optimization problem is estimated from the findings of the single objective optimization (section 4). Here, it can be considered as a preliminary study to estimate the search space for multiobjective optimization. Another justification to use this constrained search space also comes up from the limited resources of the local context in terms of the available space, and capital.

Theory and implementation of the NSGA-II (Non-dominating sorting genetic algorithm II)

Non-dominating sorting genetic algorithm II (NSGA-II) is applied for the multi-objective optimization problem and as suggested by Sohani et al. [93] that NSGA-II has several technical advantages over other techniques. The technique works on the process of natural selection in which the final breed is the best fit as compared to its ancestors. The problem is initiated based on the range of the problem along with the set of constraints. The initialized population is sorted based on the non-domination characteristics which is a measure of an individual to dominate another if its objective function is not worse than the other members and at least one of its objective functions is better than the other members. After the non-dominated sorting process, the crowding distance is assigned which is a measure of closeness of one member to its neighbor. The concept behind the assignment of crowding distance is to evaluate the Euclidian distance between the individuals and larger values of crowding distance will yield a better diversity in the population. Afterwards, the selection of the individuals is considered using a binary tournament selection with a crowded-comparison-operator. The best-fit solutions are passed on to the new generation and the worst-case scenarios are eliminated. Afterwards, the processes of mutation, cross-over, and selection are carried out and this new generation is replaced with the previously rejected members. Since all the previous and the current best individuals are added to the population, therefore, elitism is

¹ Theoretical details of the ANN architecture can be reviewed in the previous work of authors [92].

² Theoretical details of the GMDH architecture can be reviewed in the previous work of authors [92] and the one published by Sohani et al. [91].

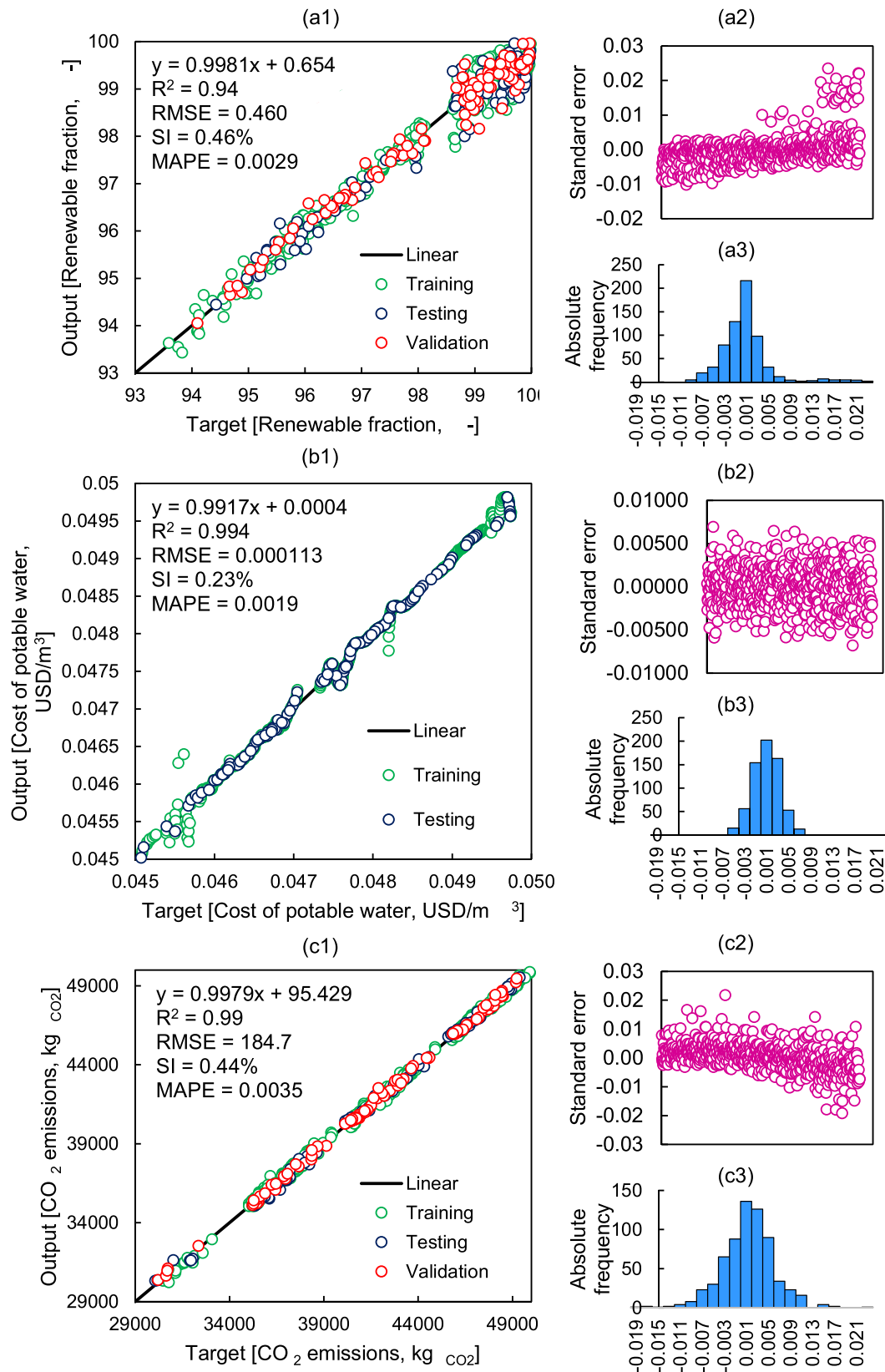


Fig. 5. (a1, b1, and c1) Comparison between the target and output performance indicator, (a2, b2, and c2) verification of independence and homoscedasticity of errors, and (c1, c2, and c3) verification of normal distribution of errors.

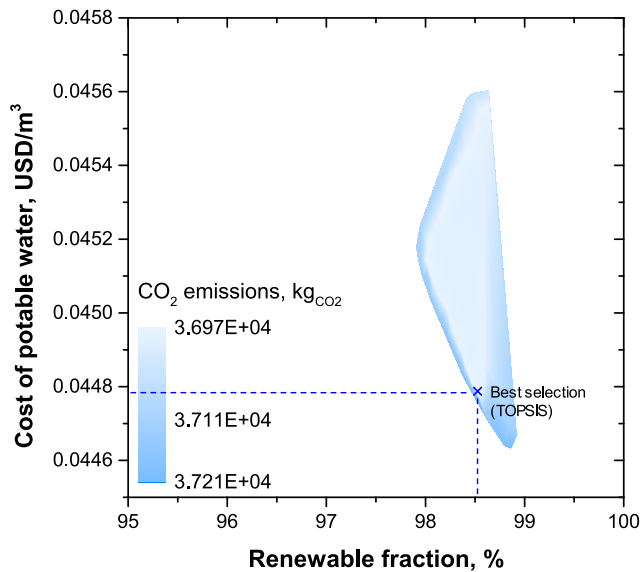


Fig. 6. Pareto front along with TOPSIS best selection of the multi-objective optimization scenario.

ensured. This process is repeated in such a way the best individuals could pass their best genes in the upcoming generations until reaching a convergence criterion. The multi-objective optimization is implemented in MATLAB global optimization toolbox [90] using the default characteristics and the flow diagram highlighting the steps for the implementation of the code is presented in Appendix D.

Multicriteria decision analysis using The Order of Preference by Similarity to Ideal Solution (TOPSIS)

Unlike the single-objective optimization, the results of multi-objective optimization are a set of non-dominating candidate solutions which is represented in a Pareto front (see Fig. 6). The final multi-objective optimization point among the Pareto front should be

evaluated using a suitable decision-making method. In this case, The Order of Preference by Similarity to Ideal Solution (TOPSIS) is adapted in which the relative distance (d_i^+ , d_i^-) of each optimized performance indicator (PI) is calculated with respect to the ideal and non-ideal solution, given by the equation:

$$d_i^+ = \sqrt{\sum_{j=1}^3 [PI_{ij} - PI_j^{\text{ideal}}]^2} \quad (11)$$

$$d_i^- = \sqrt{\sum_{j=1}^3 [PI_{ij} - PI_j^{\text{non-ideal}}]^2} \quad (12)$$

In the next step, the relative closeness of each alternative with respect to the ideal solution (d_i^+) is calculated, using the equation:

$$RC_i = \frac{d_i^-}{d_i^- + d_i^+} \quad (13)$$

The matrix of relative closeness is sorted in ascending order and a single solution with its maximum value is chosen.

Optimization results (Pareto front)

The outcome of the application of multi-objective optimization and the TOPSIS solution are presented in Fig. 6. It can be noted that the results of the multi-objective optimization are a set of solutions enclosed in the area of the performance indicators with the following range: renewable fraction ranges from 98 % to 99 %, cost of potable water ranges from ~ 0.0446 USD/m³ to ~ 0.0456 USD/m³, and the CO₂ emissions range from 36,970 kg to 37,210 kg. The best selection opted by TOPSIS is the following point on the Pareto front: the renewable fraction of 98.5 %, the cost of potable water of 0.0447 USD/m³, and the CO₂ emissions of 36,970 kg.

Comparison of optimization scenarios

In this section, the results of the spreadsheet and HOMER are compared with the multi-objective optimization scenario. The results of HOMER and spreadsheet consider the optimization scenario in which

Table 8

Concluding a comparison of the optimized performance indicators and the system capacity for various optimization scenarios.

Optimization scenario	Optimized performance indicators					System capacity			
	Cost of electricity, USD/kWh	Net present cost, USD	Renewable fraction, %	Cost of potable water, USD/m ³	CO ₂ emissions, kgCO ₂ /year	PV, kW	Generator, kW	Batteries, kWh	Inverter, kW
Optimization scenario no. 1: Min(obj) = <div style="display: flex; align-items: center;"> <div style="margin-right: 10px;"> $\begin{cases} \text{obj} : \text{Net present cost (NPC)} \\ \updownarrow \\ \text{obj} : \text{Cost of electricity (COE)} \end{cases}$ </div> <div> *Interpretation: Minimize net-present-cost (NPC) and cost of electricity (COE) through HOMER. </div> </div>	0.205	\$70,415	98.9	0.0450	–	17	5	48	6.8
Optimization scenario no. 2: Min(obj) = <div style="display: flex; align-items: center;"> <div style="margin-right: 10px;"> $\begin{cases} \text{obj} : \text{Net present cost (NPC)} \\ \updownarrow \\ \text{obj} : \text{Cost of electricity (COE)} \end{cases}$ </div> <div> *Interpretation: Minimize net-present-cost (NPC) and cost of electricity (COE) through a spreadsheet. </div> </div>	0.229	\$78,732	95.9	0.0503	–	17.7	5	44	5.3
Optimization scenario no. 3: Min(obj) = <div style="display: flex; align-items: center;"> <div style="margin-right: 10px;"> $\begin{cases} \text{obj}_1 : \text{Renewable fraction} \\ \text{obj}_2 : \text{Cost of potable water} \\ \text{obj}_3 : \text{CO}_2 \text{ emissions} \end{cases}$ </div> <div> Interpretation: Multiobjective optimization to maximize renewable fraction, minimize the cost of potable water, and minimize CO₂ emissions using surrogate (digital twin) model implemented on MATLAB. </div> </div>	0.203	\$69,895	98.5	0.0447	36,970	16.5	4	50	6.5

* Optimization scenario no. 1 and no. 2 are single-objective optimization because net present cost and the cost of electricity are linearly correlated.

Table 9

Results of sensitivity analysis. Note: *R* is the Pearson correlation coefficient. A *p*-value greater than 0.05 indicates statistical insignificance for a confidence interval of 95%. The table is symmetric at $y = -x$.

Variable	PV capacity	Generator capacity	Battery capacity	Inverter capacity	Net present cost	Cost of electricity	Renewable fraction	Cost of potable water	CO ₂ emissions
PV capacity		R=-0.1687 (p-value=0.0000)	R=0.1030 (p-value=0.0000)	R=0.0323 (p-value=0.1491)	R=-0.3354 (p-value=0.0000)	R=-0.3354 (p-value=0.0000)	R=0.4741 (p-value=0.0000)	R=-0.3355 (p-value=0.0000)	R=-0.1951 (p-value=0.0000)
Generator capacity			R=-0.2189 (p-value=0.0000)	R=0.1090 (p-value=0.0000)	R=0.1155 (p-value=0.0000)	R=0.1154 (p-value=0.0000)	R=-0.1211 (p-value=0.0000)	R=0.1154 (p-value=0.0000)	R=0.2495 (p-value=0.0000)
Battery capacity				R=0.0523 (p-value=0.0193)	R=-0.1145 (p-value=0.0000)	R=-0.1145 (p-value=0.0000)	R=0.3489 (p-value=0.0000)	R=-0.1145 (p-value=0.0000)	R=-0.1963 (p-value=0.0000)
Inverter capacity					R=-0.3709 (p-value=0.0000)	R=-0.3709 (p-value=0.0000)	R=0.3179 (p-value=0.0000)	R=-0.3710 (p-value=0.0000)	R=0.9148 (p-value=0.0000)
Net present cost						R=1.0000 (p-value=0.0000)	R=-0.9401 (p-value=0.0000)	R=1.0000 (p-value=0.0000)	R=-0.1162 (p-value=0.0000)
Cost of electricity								R=1.0000 (p-value=0.0000)	R=-0.1163 (p-value=0.0000)
Renewable fraction									R=0.0399 (p-value=0.0745)
Cost of potable water									R=-0.1163 (p-value=0.0000)
CO ₂ emissions									

the decision is carried out using only a single-objective optimization, i. e., net-present-cost and the cost of electricity are linearly correlated. However, the multi-objective optimization considered the energetic, economical, and environmental performance indicators in the form of a renewable fraction, cost of potable water, and yearly CO₂ emissions, respectively. Consequently, the perspective of the multi-objective optimization is much broader than the optimization proposed by HOMER or the one in the spreadsheet.

It can be seen in Table 8 that the performance indicators through the multi-objective optimization are more refined as compared to the other methods. It is reported that through the multi-objective optimization, the cost of electricity and the net present cost is further reduced by 0.86 % and 0.73 %, respectively at a decrement of only 0.4 % of the renewable fraction. It makes sense because even a high renewable fraction can also contribute to carbon emissions because of the emission factor of a photovoltaic system, battery storage, and inverters. In other words, a higher renewable energy fraction can move the system to an overdesign point where the emissions are high. Therefore, the results of multi-objective optimization are significant because they are based on the minimization of CO₂ emissions. Consequently, a lower renewable fraction is justified to constraint the emissions of CO₂.

Sensitivity of design variables on the objective functions

Sensitivity analysis is an assessment of the uncertainty of the design variables on the objective functions. It is used to test the robustness of the results of a model in the presence of uncertainty, development of better robust models, calibration of the theoretical model, identifying the desired optimization space, to enhance the communication from the modeling hand to the decision-makers, to simplify the model, to look for errors in the model, to reduce the uncertainty, and to understand the nature of the relationship between the input and the output variables of a system. This tool also helps to identify more responsive variables in the system.

Statistics based sensitivity analysis

In this work, a calculus [94] and statistics-based sensitivity analysis, which is reliable and fundamental in any area is carried out. Statistical

based sensitivity analysis is displayed in Table 9, which highlights the correlation of the input variables (PV capacity, inverter capacity, generator capacity, and battery storage capacity) with the output variables (net present cost, cost of electricity, renewable fraction, cost of potable water, and CO₂ emissions). Statistical-based sensitivity analysis is implemented on the software STATGRAPHICS [95]. This analysis also assists to understand the correlation and interaction between the input variables and the output variables. It can be noted that a positively correlated and statistically significant strongest correlation is noted between the cost of electricity and cost of potable water since they are linearly dependent while being a function only of the net present cost. It is followed by a renewable fraction with the cost of potable water which is rational because a very high renewable fraction can also correspond to the high cost of renewable energy equipment which yields a rise in the cost of potable water. Similarly, there is a positive correlation between the generator and inverter capacity with the CO₂ emissions, and it corresponds to the fact that the increment in the size of the generator and inverter would contribute towards the life cycle CO₂ emissions. The statistically significant negatively correlated is noted between the net present cost and cost of electricity with the renewable fraction signifying that a very high net present cost and cost of electricity corresponds to high usage of diesel generators, resulting in a lower renewable fraction. However, there is one drawback of this statistical-based sensitivity analysis: although it exhibits the relationship between the variables, it does not exhibit the sensitivity of the model with respect to any uncertainty in the design variables. Therefore, calculus-based sensitivity analysis is reported here to further extend the analysis.

Calculus-based (partial derivative-based) sensitivity analysis

The calculus-based sensitivity method considers the summation of each design variable and its respective uncertainty, which can be expressed as follows [96]:

$$X = \bar{X} \pm \hat{U}_x \quad (14)$$

In eq. (14), *X* is the design variable, which can be PV capacity, inverter capacity, generator capacity, or battery capacity. \bar{X} is its nominal value, and $\pm \hat{U}_x$ is the possible uncertainty in the nominal value of

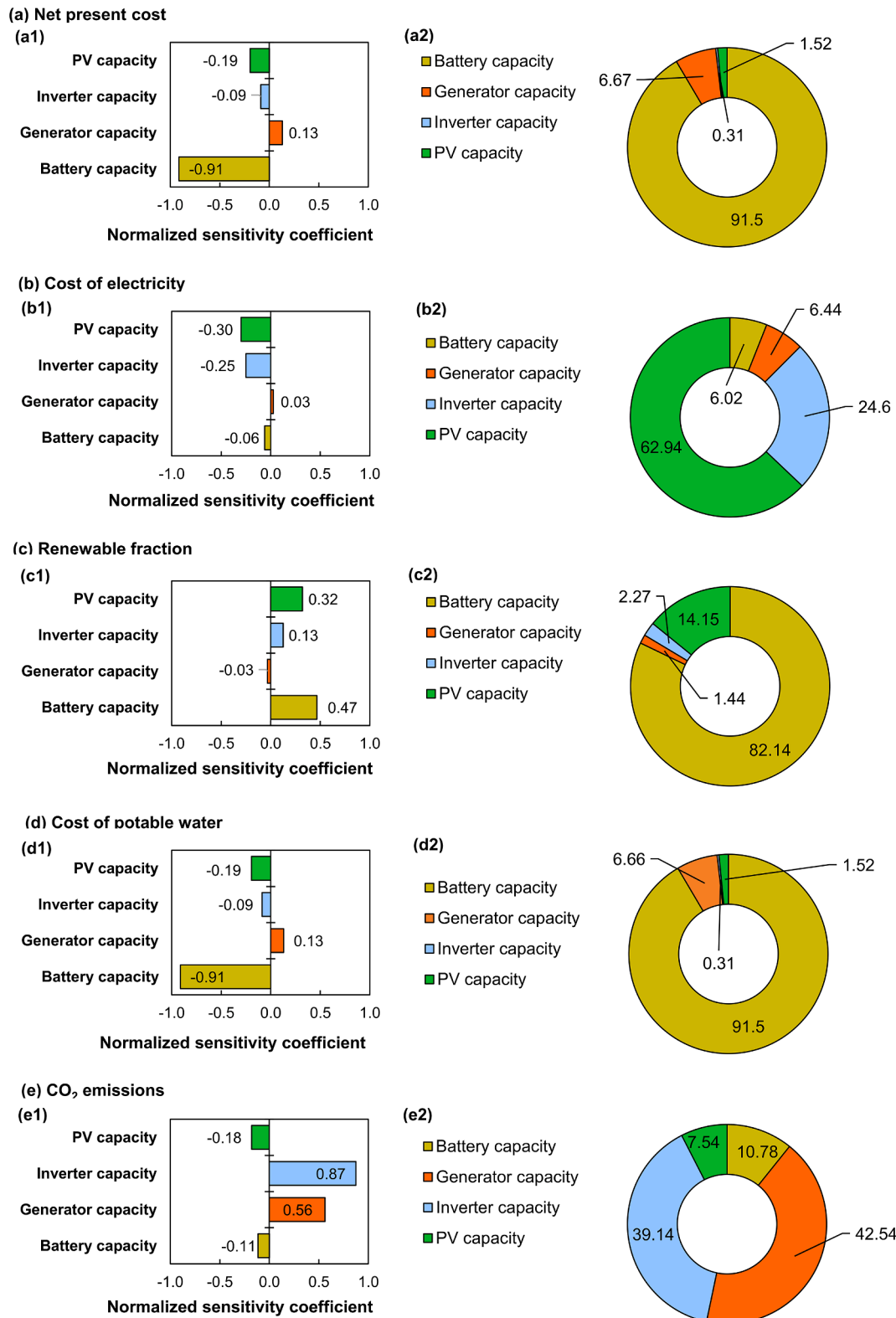


Fig. 7. Results of sensitivity analysis including normalized sensitivity coefficient and relative sensitivity coefficient for (a) net present cost, (b) cost of electricity, (c) Renewable fraction, (d) cost of potable water, and (e) CO₂ emissions.

the design variable [97]. This method expresses the corresponding uncertainty in the objective function owing to the uncertainty in the design variable, which can be written as:

$$\hat{U}_Y = \frac{dY}{dX} \hat{U}_x \quad (15)$$

In eq. (15), \hat{U}_Y represents the uncertainty in any Y objective function, which can be net present cost, cost of electricity, renewable fraction, cost of potable water, and/or CO₂ emissions. The term $\frac{dY}{dX}$ represents the change in the objective function Y with respect to the set of design variables X . Therefore, in such multivariate problems, the uncertainty in

Table 10
Comparison of different results about hybrid renewable energy systems in the literature.

Research study	Hybrid system component	Load detail	Sizing Approach	Results of sizing			Overview
				Technical indicators	Economic indicators	Environmental indicators	
[43]	PV, Energy Storage (ES), DG, Hydro, BESS	24.4 kW total	HOMER	PV: 332 kW ES: 3 kW BESS: 1100 kWh	NPC: 465,790 USD COE: 0.10 USD/kWh	CO ₂ emissions: 20,868 kg/yr	This research study is carried out to analyze the provide power supply using an HRES for a remote rural area in the state of Karnataka (India) with a combined dispatch strategy.
[103]	PV, ES, Pumped hydro storage (PHS)	255.6 kWh/day total	Particle Swarm Optimization	PV: 84 kW ES: 75 kW PHS: 320 kWh	COE: 0.196 USD/kWh	Unspecified	This study investigates and compares the various combinations of renewable energies (solar, wind) and storage technologies (battery, pumped hydro storage, hybrid storage) for an off-grid power supply system.
[39]	PV, ES, Biogas generator (BGG), biomass generator (BMG), Battery Energy Storage System (BESS), and fuel cell	724.83 kWh/day total 149.21 kW peak	GA HOMER	PV: 100 kW ES: 50 unities BESS: 200 unities BGG: 60 kW BMG: 50 kW Fuel cell: 57 kW Electrolyzer: 50 kW	NPC: 890,013 USD COE: 0.163 USD/kWh	CO ₂ emissions: 3,842 kg/yr	This work compares two methods to find the best optimal solution of NPC, COE, and CO ₂ emissions of an HRES.
[104]	PV, ES, DG, BESS	3000 kW peak/yr	Multi-Objective Self-Adaptive Differential Evolution (MOSaDE)	PV: 40.4 kW ES: 10 kW	COE: 0.050 USD/kWh	RF: 95.18 %	This paper conducts the optimal sizing of a PV/ES/DG with battery storage using the Multi-Objective Self-Adaptive Differential Evolution (MOSaDE) algorithm for the city of Yanbu, Saudi Arabia.
[44]	PV, ES, DG, BESS	200 kW average	HOMER	PV: 200 kW ES: 200 kW DG: 365 kW BESS: 150 kWh	NPC: 3,677,573 USD COE: 0.751 USD/kWh	CO ₂ emissions: 314.6 Tons/yr	This research study develops an economical and technical feasibility method to determine the best implementation of a novel energy storage system in an HRES.
[105]	PV, DG, Grid	30 kW base 758 kW peak	HOMER	PV: 200 kW Grid: 850 kW	NPC: 3,336,403 USD COE: 0.130 USD/kWh	RF: 18 %	This work investigates the optimization of several hybrid energy system models consisting of solar PV, diesel generators, and grid.
[106]	PV, ES; BMG, BGG, Hydro, BESS	2,434,500 kWh/yr	Genetic algorithm (GA)	Hydro: 16 kW BMG: 77 kW BGG: 50 kW ES: 49 kW BESS: 936 kVA	NPC: 605,376 USD COE: 0.087 USD/kWh	Unspecified	The present work focuses on the optimal sizing of an integrated renewable energy system considering locally available different renewable energy sources for electrification of a remote area in Karnataka state in India.
[45]	PV, ES, BESS, BGG	54 kWh/day average	HOMER	PV: 1 kW ES: 1 kW BGG: 2 kW BESS: 2.16 kWh	NPC: 72,232 USD COE: 0.306 USD/kWh	CO ₂ emissions: 26,894 kg/yr RF: 100 %	This paper presents an economic feasibility analysis of a single standalone house operating with a hybrid power plant consisting of a fixed capacity producer gas generator and other renewable energy sources (PV and ES).
[46]	PV, ES, DG, BESS	33 kWh/day 3.9 kW peak	HOMER	PV: 18 kW ES: 20 kW DG: 3 kW BESS: 25 unities	NPC: 288,194 USD COE: 1.877 USD/kWh	CO ₂ emissions: 198,347.9 kTons/yr RF: 66.3 %	This study is carried out to analyze the performance of an off-grid/PV/ES/DG/BESS hybrid energy system for a remote area in Malaysia.
[47]	PV, BESS, DG, BMG, BGG, Micro-hydro generator (MHG)	100 kW peak	Particle Swarm Optimization GA Biogeography techniques	PV: 56 kW BESS: 110 kVA BMG: 30 kW BGG: 35 kW DG: 30 kW MHG: 15 kW	COE: 0.077 USD/kWh	CO ₂ emissions: 14,614 kg/yr RF: 96 %	The present work includes sizing of hybrid energy systems using various energy management strategies which are the cycle charging strategy, load following strategy, and peak shaving strategy.
Present study	PV, ES, DG, BESS	4.25 kW maximum 74.09 kWh/day	Spreadsheet ANN HOMER	PV: 16.5 kW DG: 4 kW BESS: 50 kWh Power Converter: 6.5 kW	NPC: 69,895.6 USD COE: 0.2032 USD/kWh Cost of potable water:	CO ₂ emissions: 36,970 kg/yr RF: 98.5 %	This research study aims to evaluate the technical and economic indicators of different HRES to satisfy the energy demand of two water treatment plants in a remote community in the state of

(continued on next page)

Table 10 (continued)

Research study	Hybrid system component	Load detail	Sizing Approach	Results of sizing			Overview
				Technical indicators	Economic indicators	Environmental indicators	
					0.0447 USD/m ³		Yucatan by using artificial intelligence and HOMER.

Abbreviations and/or acronyms: PV: photovoltaic panels, ES: energy storage, DG: diesel generator, Hydro: Hydropower, BESS: battery energy storage system, HOMER: Hybrid Optimization of Multiple Energy Resources, NPC: net present cost, COE: cost of energy, HRES: hybrid renewable energy systems, PHS: pumped hydro storage, BGG: biogas generator, BMG: biomass generator, GA: genetic algorithm, MOSaDE: Multi-Objective Self-Adaptive Differential Evolution, RF: renewable factor, MHG: micro-hydro generator.

Y with respect to the perturbations in X are calculated as the root sum square product of each individual perturbation [98]. It is expressed in the following equation:

$$\hat{U}_Y = \sqrt{\sum_{\text{first objective function}}^{\text{last objective function}} \left[\left(\frac{dY}{dX_{\text{objective function}}} \hat{U}_{x,\text{objective function}} \right)^2 \right]} \quad (16)$$

Another suitable option is to report the results of the sensitivity analysis through Normalized Sensitivity Coefficients (NSC) which is attained through the normalization of the uncertainty \hat{U}_Y by dividing it with the nominal value of the objective function [99]. Thus, it can be written as:

$$\frac{\hat{U}_Y}{\bar{Y}} = \sqrt{\sum_{\text{first objective function}}^{\text{last objective function}} \left[\left(\frac{dY_{\text{objective function}}}{dX_{\text{objective function}}} \times \frac{\bar{X}_{\text{objective function}}}{\bar{Y}_{\text{objective function}}} \right)^2 \left(\frac{\hat{U}_{x,\text{objective function}}}{\bar{X}_{\text{objective function}}} \right)^2 \right]} \quad (17)$$

Summarizing all the information, the normalized value of the sensitivity analysis of just the Net present cost (NPC) can be written as:

$$\begin{aligned} \frac{\hat{U}_{NPC}}{\bar{NPC}} = & \sqrt{\left(\frac{dNPC}{d(PV \text{ capacity})} \times \frac{PV \text{ capacity}}{\bar{NPC}} \right)^2 \left(\frac{\hat{U}_{PV \text{ capacity}}}{\bar{PV \text{ capacity}}} \right)^2 + \left(\frac{dNPC}{d(Generator \text{ capacity})} \times \frac{Generator \text{ capacity}}{\bar{NPC}} \right)^2 \left(\frac{\hat{U}_{Generator \text{ capacity}}}{\bar{Generator \text{ capacity}}} \right)^2} \\ & + \left(\frac{dNPC}{d(Battery \text{ capacity})} \times \frac{Battery \text{ capacity}}{\bar{NPC}} \right)^2 \left(\frac{\hat{U}_{Battery \text{ capacity}}}{\bar{Battery \text{ capacity}}} \right)^2 + \left(\frac{dNPC}{d(Inverter \text{ capacity})} \times \frac{Inverter \text{ capacity}}{\bar{NPC}} \right)^2 \left(\frac{\hat{U}_{Inverter \text{ capacity}}}{\bar{Inverter \text{ capacity}}} \right)^2 \end{aligned} \quad (18)$$

Once these parameters are evaluated, a relative sensitivity coefficient can be estimated to identify the dominant contributors among the design variables towards the objective functions. Mathematically, it is calculated by multiplying the sensitivity coefficient and uncertainty normalized by the uncertainty in the objective function accompanied by the square of the whole equation [100]. Thus, it can be written as:

$$RSC = \left(\frac{\frac{dY}{dX} \hat{U}_x}{\hat{U}_Y} \right)^2 \quad (19)$$

In eq. (19), RSC is the relative sensitivity coefficient and the

summation of RSC's for a particular objective function for all the design variables is equal to 1 (or 100%).

Calculus-based sensitivity analysis is applied on Engineering Equation Solver (EES) using the toolbox "Uncertainty Propagation" [101]. The results of the derivate-based sensitivity analysis are reported in Fig. 7. It can be noted from Fig. 7(a1, b1, and d1) that the uncertainty of change in the PV capacity, inverter capacity, and battery capacity would bring down the net present cost, cost of electricity, and cost of potable water. Practically, it is also reasonable, besides, it also complies with the findings of Table 9, where the energy load is constant. Therefore, an increase in these design variables would techno-economically justify the renewable energy components in this hybrid energy system. However, it can also be noted from the same figures that the uncertainty of change in

the generator capacity would increase the net present cost, cost of electricity, and the cost of potable water since the diesel generator would be using an expensive resource (diesel) instead of exploiting

freely available solar energy. The findings of Fig. 7(c1) illustrate that the renewable energy components of this hybrid system including solar panels, inverters, and batteries are contributing positively towards the renewable fraction, whereas, the generator pulls down this renewable fraction. The interpretation of Fig. 7(e1) and the last column of Table 9 are somewhat challenging where apparently it seems like only the inverter and the generator are contributing positively towards the environmental emissions, whereas incrementing solar panels and batteries lowers the environmental emissions. It is explained through the concept that the design variables are also correlated. Therefore, an increase in the PV capacity would yield a decrease in the generator capacity to meet the same energy load. Since the CO₂ emissions of batteries

and solar panels are lower than the other components [82–84]. Therefore, it seems that the inverter and generator are contributing positively in this case. In summary, the net present cost, renewable fraction, and cost of potable water are strongly correlated with the battery size (Fig. 7 (a2, c2, and d2)). Similarly, the most sensitive parameter for the cost of electricity and the CO₂ emissions are solar panels and diesel generators, respectively (Fig. 7(b2, and e2)).

Comparison of results with external literature

It is possible to find different works related to this research study in the current literature, which tend to optimize energetic, economic, and environmental indicators from the hybrid renewable energy system proposed for the corresponding application. In Table 10, a summary of the results obtained by different authors is presented.

As seen from Table 10, COE results are reported between 0.050 USD/kWh and 1.877 USD/kWh, and NPC between 72,232 USD and 3,677,573 USD. In this study, an optimized COE of 0.2032 USD/kWh was obtained, which is within the range of values reported in Table 8. However, the value of the NPC is lower than the results from the literature. This is attributed to the daily energy demand of this study, which was 79.06 kWh/day, with a maximum demand of 4.25 kW. When comparing this value with the one reported by [39], there is an energy demand of 724.83 kWh/day and an NPC of 890,013 USD. Thus, it is observed from Table 10 that the installed capacity is much higher than the reported in this work, which would lead to an increase in capital costs, O&M, and replacement costs during the entire useful life of the project.

Similarly, two important environmental indicators are CO₂ emissions and renewable fraction. The value of CO₂ emissions obtained in this work was 36,970 kg/yr, and when comparing this result with Table 10, it is observed that there are several similar values reported in the literature [48,50]. Moreover, the renewable fraction of this study was 98.5 %, and according to Table 10 values up to 100 %, a renewable fraction are reported. It should be clarified that these values depend on the percentage of participation of renewable sources within the hybrid system. Finally, the present study reported a cost for potable water and energy obtained by the optimized hybrid renewable energy systems. However, the indigenous Mayan community already has an established cost for these resources, obtained by conventional methods, so it is important to compare the costs obtained in this work with the ones that already exist.

Regarding the cost of energy, the Federal Electricity Commission (CFE, by its acronym in Spanish) is the Mexican entity in charge of supplying energy to the country. Considering the region where San Jose Tipceh has located as well as the industrial use that will be given to the energy, the corresponding energy cost is labeled as high demand in ordinary medium voltage. For this energy tariff and considering the costs published by CFE for January 2021, the COE is 0.07245 USD/kWh, with a monthly fixed charge of 27.18 USD and distribution and capacity charges of 4.66 USD/kW and 13.56 USD/kW, respectively [102]. This COE from CFE is better in comparison with the results obtained from the hybrid renewable energy systems. However, the Mayan community does not have the electrical infrastructure needed to supply the energy for high demand in ordinary medium voltage consumers, which in this case would be the water treatment plants.

Likewise, regarding the cost for potable water, the Yucatan Board of Water Supply and Sewerage (JAPAY, by its acronym in Spanish) is the public organization dedicated to the administration, operation, conservation, expansion, and construction of potable water systems in the State of Yucatan, and the cost of water is 0.36 USD/m³ [54]. When comparing this value with the one obtained in this work, there is a difference of 0.3153 USD/m³ favoring the hybrid energy system. This is attributed to

the fact that the distribution comes from a water treatment plant which can be considered private and does not involve other costs that JAPAY considers, such as operation, pumping, expansion of the distribution system, among others. Moreover, this water does not go through the processes needed for the water to be potable, as it just serves for cleaning purposes.

Conclusion

In the present work, different configurations were analyzed for the sizing of hybrid renewable energy systems proposed for supplying the energy demanded from a water purification system suggested for installation in the indigenous Mayan community of San Jose Tipceh located in Yucatan, Mexico [107]. The technologies considered for the different configurations of the hybrid systems were photovoltaic modules, wind turbines, diesel generators, and a storage energy system with Pb-acid, Li-on, and AGM as alternatives for the battery selection. The sizing process was performed using a spreadsheet developed by the authors of this work, as well as with the software HOMER pro. The main criteria considered for the selection of the hybrid systems were the economic indicators of net present cost and cost of energy. For both techniques used for the sizing process, the results indicated that the best hybrid system comprised of photovoltaic technology with a diesel generator and a storage energy system with Li-ion batteries. The values obtained with HOMER for the NPC and COE were 70,415 USD and 0.205 USD/kWh, while those obtained with the spreadsheet were 78,732 USD and 0.229 USD/kWh, respectively. Moreover, the renewable fraction was 98.5 % obtained from HOMER, while from the spreadsheet it was 95.9 %. Additionally, the potable water costs were 0.0450 USD/m³ and 0.0503 USD/m³ for HOMER and the spreadsheet, respectively. Regarding the results obtained from the multi-objective optimization, it was found that the NPC and the COE were 69,895 USD and 0.203 USD/kWh, respectively, which represents a lower value than the results from HOMER with a difference of 500 USD for the NPC and 0.002 USD/kWh for the COE. Moreover, the cost of potable water was optimized and a value of 0.0447 USD/m³ was obtained, while the renewable fraction was 98.5 % and the total CO₂ emission was 36,970 kgCO₂/year. Finally, these results were compared with results obtained by different authors, confirming that the present study lies in the context of recent research literature and makes it suitable for the sizing and optimization of hybrid renewable energy systems.

There are certain advantages and disadvantages to the adapted method. One of the advantages is that the usage of spreadsheet algorithms offers computationally cheap, and reliable results as compared to the usage of licensed HOMER pro which is equally reliable for single-objective optimization scenarios. Another advantage of this method is that the multiobjective optimization adds certain features to the HOMER pro and spreadsheet algorithm by including the environmental and water cost. One of the drawbacks of the usage of multiobjective optimization is that it's computationally expensive as compared to spreadsheet algorithms since it involves an intermittent step of the generation of the digital twin. As a precautionary measure, extensive validation should be accomplished before using any digital twin for the multi-objective optimization because they are vulnerable to several numerical errors. Additionally, the operational range of the digital twin should be big enough to cover the search space of the optimization results. Otherwise, the optimization procedure can also extrapolate the surrogate model which would lead to uninterpretable findings.

Finally, the lack of proper water and wastewater treatment infrastructure in isolated rural areas like the one studied must be addressed in order to guarantee water safety for the future. Hence, it is highly desired to incorporate economically feasible technologies from an energetic

point of view such as HRES. The design, techno-economic optimization, and sensitivity analysis of such a water management plant are reported in this article. At the next step, a feasibility study should also consider the societal and governmental constraints. For instance, social rejection is a pivotal factor to acknowledge since resistance towards renewable energy megaprojects in Yucatan, Mexico, by the indigenous community has been previously demonstrated by El-Mekkaoui et al. [107]. Consequently, it is important to consider that the implementation of technologies such as the proposed water management system should be carried out in harmony with the beliefs, culture, and lifestyle of the targeted communities.

CRediT authorship contribution statement

Rasikh Tariq: Conceptualization, Methodology, Software, Validation, Formal analysis, Investigation, Resources, Data curation, Writing – original draft, Writing – review & editing, Visualization, Supervision, Project administration. **A.J. Cetina-Quinones:** Conceptualization, Methodology, Software, Validation, Formal analysis, Investigation, Resources, Data curation, Writing – original draft, Writing – review & editing, Visualization, Project administration. **V. Cardoso-Fernández:** Conceptualization, Methodology, Software, Formal analysis, Investigation, Resources, Data curation, Writing – original draft, Writing – review & editing, Visualization, Project administration. **Hernández-López Daniela-Abigail:** Methodology, Software, Formal analysis, Resources, Data curation, Writing – original draft, Writing – review & editing. **M. A. Escalante Soberanis:** Conceptualization, Methodology, Software, Validation, Resources, Writing – review & editing, Visualization, Supervision, Project administration, Funding acquisition. **A. Bassam:**

Methodology, Validation, Resources, Writing – review & editing, Supervision, Project administration, Funding acquisition. **M. Vega De Lille:** Methodology, Validation, Resources, Writing – review & editing, Supervision, Project administration, Funding acquisition.

Declaration of Competing Interest

The authors declare that they have no known competing financial interests or personal relationships that could have appeared to influence the work reported in this paper.

Acknowledgment

The authors, Rasikh Tariq, A.J. Cetina-Quinones, V. Cardoso Fernández, and Daniela Abigail Hernandez Lopez, are grateful to the financial support of CONACYT (*Consejo Nacional de Ciencia y Tecnología*) to pursue a postgraduate degree in *Facultad de Ingeniería, Universidad Autónoma de Yucatán* under the following details: (a) Rasikh Tariq, CVU: 949314, scholarship no: 784785; (b) A.J. Cetina-Quinones, CVU: 861995, scholarship no: 784880; (c) V. Cardoso Fernández, CVU: 1006703, scholarship no: 752330, and (d) Daniela Abigail Hernández López, CVU: 1007727, scholarship no: 752354.

Appendix A. Annual total load and total power output of optimized hybrid energy system

See Fig. A1

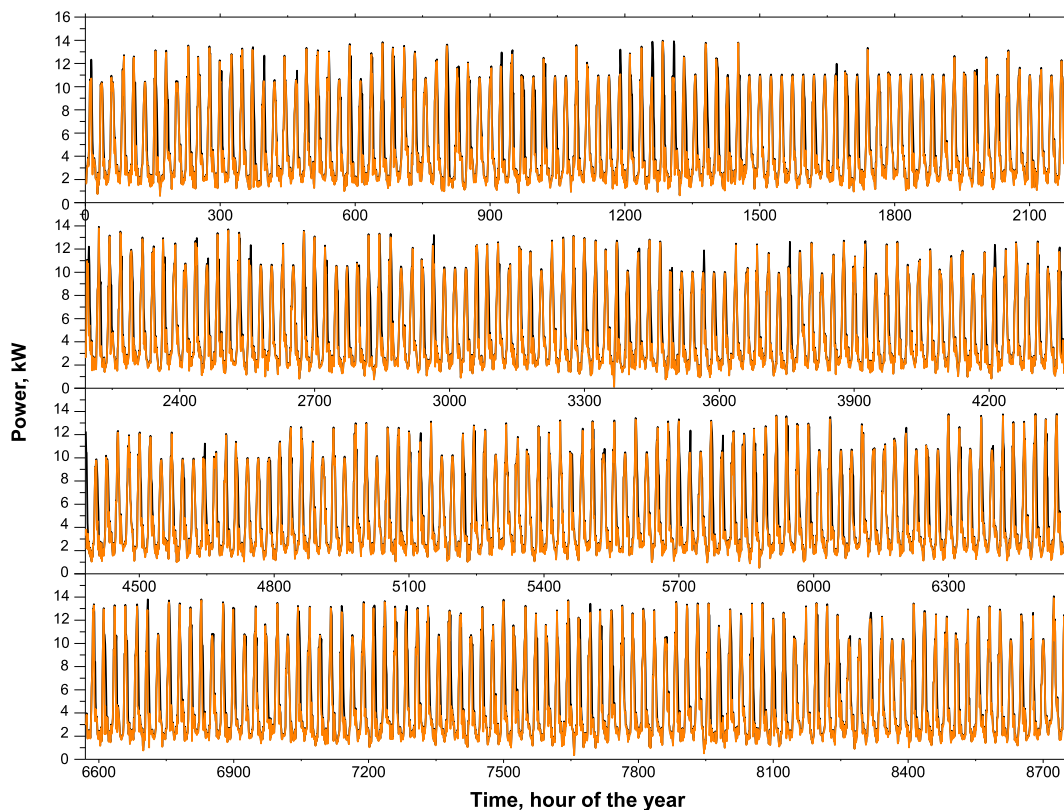


Fig. A1. Annual total load and total power output of the optimized hybrid energy system (case 4: PV/DG/BESS with Li-ion battery storage, see Table 6) displaying the pattern for each hour of the whole year. Note: Each individual graph in this figure exhibits a time frame of 3 months, thus, four figures correspond to the simulation of the whole year. It can be observed that the peaks of total output is higher than the total load and their difference corresponds to the excess energy production.

Appendix B. Performance indicators of the regression fit

See Table B1.

Table B1
Performance indicators of regression fit.

Indicator	Formula	Description	Significance
Coefficient of determination (R^2)	$R^2 = 1 - \frac{\sum_{i=1}^N (PI_{actual} - PI_{predicted})^2}{\sum_{i=1}^N (PI_{actual} - \bar{PI}_{actual})^2}$	The coefficient of determination refers to the closeness of the fitted data. PI_{actual} corresponds to the actual performance index, $PI_{predicted}$ refers to the predicted performance index from the regression method, and \bar{PI}_{actual} is the average value of the actual performance index.	An R^2 value close to unity refers that the regression quality is high.
Mean Squared Error (MSE)	$MSE = \frac{1}{N} \sum_{i=1}^N (PI_{actual} - PI_{predicted})^2$	This coefficient is a measure of the average of the square of the errors.	The values of mean square error close to zero are suitable for the regression analysis.
Root Mean Square Error (RMSE)	$RMSE = \sqrt{\frac{\sum_{i=1}^N (PI_{actual} - PI_{predicted})^2}{N}}$	It is the standard deviation of the residuals; thus, indicating the spread of the residuals far from the regression line.	Like the MSE, a root-mean-square error near zero corresponds to the perfect regression analysis.
Scatter Index (SI)	$SI = 100 \times \frac{RMSE}{\left[\sum_{i=1}^N PI_{predicted} \right] / N}$	It presents the percentage of root-mean-square difference with respect to mean observation or it gives the percentage of expected error for the parameter [108].	A scatter index of less than 5% is considered as a strong relation.

Appendix C. External validation of digital twins

This procedure further extends the reliability of the meta-model. The motivation to carry out this validation is that a multivariate regression can often yield a biased high R^2 owing to the availability of many tuning parameters. Additionally, several researchers consider that R^2 is not sufficient proof of high predictive properties [109] of the neural fit. Consequently, external validation is conducted using the method presented by Tariq et al. [92] and Tzuc et al. [72]. It is determined by the correlation fit between the experimental and the predicted data which should range between 0.85 and 1.15. Similarly, the external predictability indicator should be less than 0.5. The correlations with the criteria implemented on the digital twins are shown in Table C1. I. It can be noted that the developed digital twins satisfy all the conditions of external validation.

Table C1
External validation statistical criteria of the digital twin.

Statistical criteria	Condition	The digital twin of:		
		Renewable fraction	Cost of potable water	CO ₂ emissions
R^2	$R^2 \geq 0.64$	0.94	0.994	0.99
$a = \frac{\sum_{i=1}^{no\ of\ data} PI_{actual}^i \cdot PI_{predicted}^i}{\sum_{i=1}^{no\ of\ data} (PI_{predicted}^i)^2}$	$0.85 \leq a \leq 1.15$	0.9998	1.0000	1.0003
$a' = \frac{\sum_{i=1}^{no\ of\ data} PI_{actual}^i \cdot PI_{predicted}^i}{\sum_{i=1}^{no\ of\ data} (PI_{actual}^i)^2}$	$0.85 \leq a' \leq 1.15$	1.0001	1.0000	0.9997
$R_o^2 = 1 - \frac{\sum_{i=1}^{no\ of\ data} (PI_{predicted}^i - a \cdot PI_{predicted}^i)^2}{\sum_{i=1}^{no\ of\ data} (PI_{predicted}^i - \bar{PI}_{predicted})^2}$	–	0.9999	1.0000	1.0000
$R_u^2 = 1 - \frac{\sum_{i=1}^{no\ of\ data} (PI_{actual}^i - a' \cdot PI_{actual}^i)^2}{\sum_{i=1}^{no\ of\ data} (PI_{actual}^i - \bar{PI}_{actual})^2}$	–	0.9999	1.0000	1.0000
$R_m = R^2 \left(1 - \sqrt{ R^2 - R_o^2 } \right)$	$R_m \geq 0.50$	0.7099	0.7097	0.7098
$m = \frac{R^2 - R_o^2}{R^2}$	$ m < 0.10$	–0.0637	–0.0638	–0.0638
$m' = \frac{R^2 - R_u^2}{R^2}$	$ m' < 0.10$	–0.0637	–0.0638	–0.0638
All the conditions are satisfied?		Yes	Yes	Yes

Appendix D.: Genetic algorithm-based multi-objective optimization

See Fig. D.1.

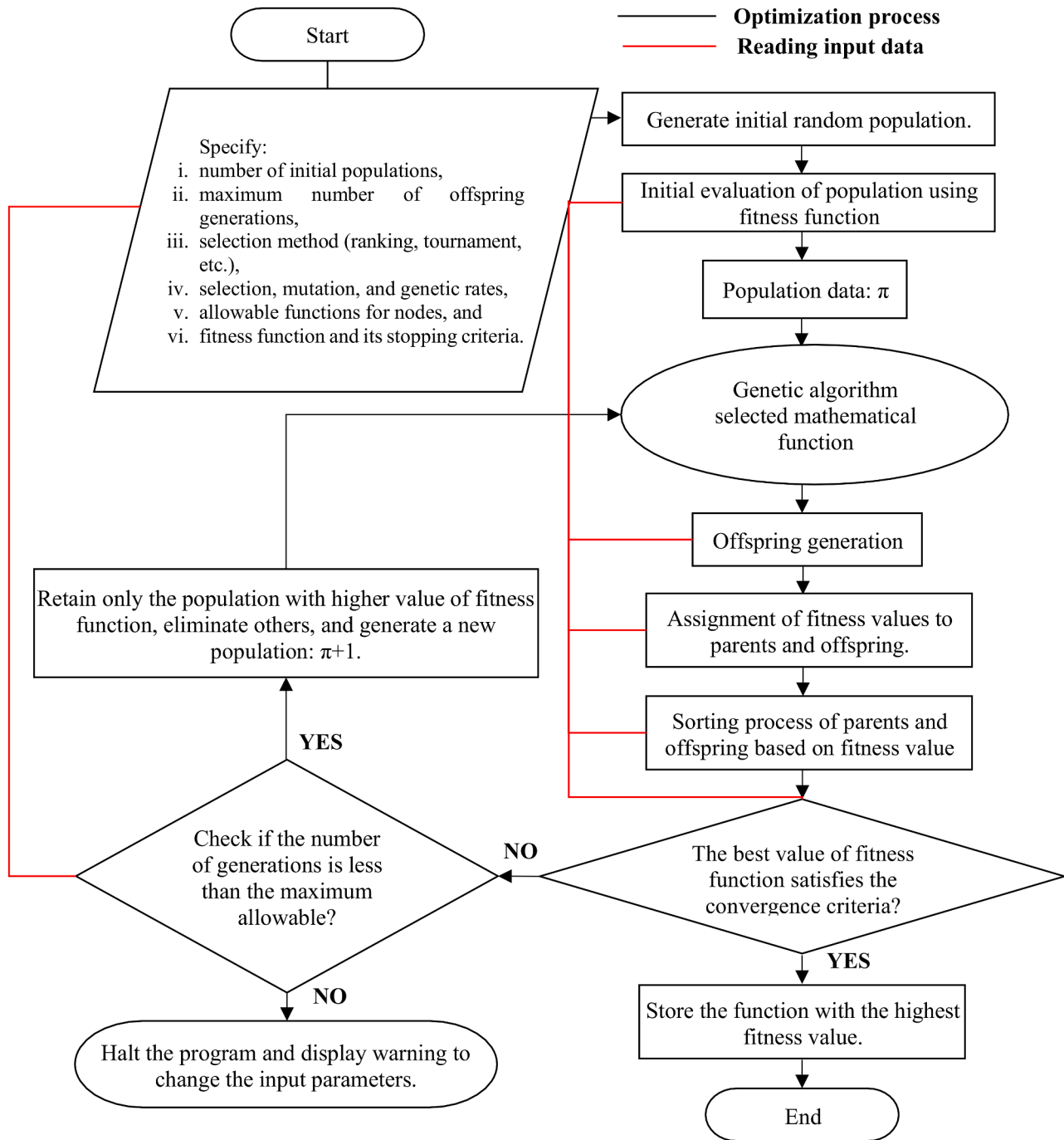


Fig. D.1. The methodology diagram opted for multi-objective optimization using a genetic algorithm.

References

- [1] Bahar R, Ng KC. Fresh water production by membrane distillation (MD) using marine engine's waste heat. *Sustain Energy Technol Assessments* 2020;42: 100860. <https://doi.org/10.1016/j.seta.2020.100860>.
- [2] Tariq R, Sheikh NA, Livas-García A, Xamán J, Bassam A, Maisotsenko V. Projecting global water footprints diminution of a dew-point cooling system: sustainability approach assisted with energetic and economic assessment. *Renew Sustain Energy Rev* 2021;140. <https://doi.org/10.1016/j.rser.2021.110741>.
- [3] Vasistha P, Ganguly R. Water quality assessment of natural lakes and its importance: an overview. *Mater Today Proc* 2020;9. <https://doi.org/10.1016/j.matpr.2020.02.092>.
- [4] Tariq R, Sheikh NA, Xamán J, Bassam A. An innovative air saturator for humidification-dehumidification desalination application. *Appl Energy* 2018; 228:789–807. <https://doi.org/10.1016/j.apenergy.2018.06.135>.
- [5] Pourmoosavi MA, Amraee T, Firuzabad MF. Expansion planning of generation technologies in electric energy systems under water use constraints with

- renewable resources. *Sustain Energy Technol Assessments* 2021;43:100828. <https://doi.org/10.1016/j.seta.2020.100828>.
- [6] Ogbolumani OA, Nwulu NI. Multi-objective optimisation of constrained food-energy-water-nexus systems for sustainable resource allocation. *Sustain Energy Technol Assessments* 2021;44:100967. <https://doi.org/10.1016/j.seta.2020.100967>.
 - [7] Sharon H. Energy, exergy and enviro-economic assessment of productivity enhanced passive double sided vertical convection solar distiller for fresh water production. *Sustain Energy Technol Assessments* 2020;42:100846. <https://doi.org/10.1016/j.seta.2020.100846>.
 - [8] Essa FA, Elsheikh AH, Sathyamurthy R, Muthu Manokar A, Kandeal AW, Shanmugan S, et al. Extracting water content from the ambient air in a double-slope half-cylindrical basin solar still using silica gel under Egyptian conditions. *Sustain Energy Technol Assessments* 2020;39:100712. <https://doi.org/10.1016/j.seta.2020.100712>.
 - [9] Zehetbiyan-Rezaie N, Alvandifar N, Saffaravai F, Makkiabadi M, Rahmati N, Saffar-Avval M. A solar-powered solution for water shortage problem in arid and semi-arid regions in coastal countries. *Sustain Energy Technol Assessments* 2019; 35:1–11. <https://doi.org/10.1016/j.seta.2019.05.015>.
 - [10] Vilanova MRN, Balestieri JAP. Energy and hydraulic efficiency in conventional water supply systems. *Renew Sustain Energy Rev* 2014;30:701–14.
 - [11] Tariq R, Sheikh NANA, Bassam A, Xamán J. Analysis of Maisotsenko humid air bottoming cycle employing mixed flow air saturator. *Heat Mass Transf* 2018;55. <https://doi.org/10.1007/s00231-018-2531-z>.
 - [12] Tariq R, Sheikh NA. Numerical heat transfer analysis of Maisotsenko Humid Air Bottoming Cycle – a study towards the optimization of the air-water mixture at bottoming turbine inlet. *Appl Therm Eng* 2018;133:49–60. <https://doi.org/10.1016/j.applthermaleng.2018.01.024>.
 - [13] Temiz M, Dincer I. Enhancement of solar energy use by an integrated system for five useful outputs: System assessment. *Sustain Energy Technol Assessments* 2021;43:100952. <https://doi.org/10.1016/j.seta.2020.100952>.
 - [14] Noorollahi Y, Khatibi A, Eslami S. Replacing natural gas with solar and wind energy to supply the thermal demand of buildings in Iran: A simulation approach. *Sustain Energy Technol Assessments* 2021;44:101047. <https://doi.org/10.1016/j.seta.2021.101047>.
 - [15] Agyekum EB, Velkin VI, Hossain I. Sustainable energy: is it nuclear or solar for African Countries? Case study on Ghana. *Sustain Energy Technol Assessments* 2020;37:100630. <https://doi.org/10.1016/j.seta.2020.100630>.
 - [16] Tariq R, Zhan C, Zhao X, Sheikh NA. Numerical study of a regenerative counter flow evaporative cooler using alumina nanoparticles in wet channel. *Energy Build* 2018;169:430–43. <https://doi.org/10.1016/j.enbuild.2018.03.086>.
 - [17] Tariq R, Sheikh NA, Xamán J, Bassam A. Recovering waste energy in an indirect evaporative cooler – a case for combined space air conditioning for human occupants and produce commodities. *Build Environ* 2019;152:105–21. <https://doi.org/10.1016/j.buildenv.2019.01.038>.
 - [18] Tariq R, Zhan C, Ahmed Sheikh N, Zhao X. Thermal performance enhancement of a cross-flow-type maisotsenko heat and mass exchanger using various nanofluids. *Energies* 2018;11:2656. <https://doi.org/10.3390/en1102656>.
 - [19] Carvajal-Romo G, Valderrama-Mendoza M, Rodríguez-Urrego D, Rodríguez-Urrego L. Assessment of solar and wind energy potential in La Guajira, Colombia: Current status, and future prospects. *Sustain Energy Technol Assessments* 2019; 36:100531. <https://doi.org/10.1016/j.seta.2019.100531>.
 - [20] Raghuwanshi SS, Arya R. Reliability evaluation of stand-alone hybrid photovoltaic energy system for rural healthcare centre. *Sustain Energy Technol Assessments* 2020;37:100624. <https://doi.org/10.1016/j.seta.2019.100624>.
 - [21] Ben Ali I, Turki M, Belhadj J, Roboam X. Systemic design and energy management of a standalone battery-less PV/Wind driven brackish water reverse osmosis desalination system. *Sustain Energy Technol Assessments* 2020;42: 100884. <https://doi.org/10.1016/j.seta.2020.100884>.
 - [22] Jahangir MH, Cheraghi R. Economic and environmental assessment of solar-wind-biomass hybrid renewable energy system supplying rural settlement load. *Sustain Energy Technol Assessments* 2020;42:100895. <https://doi.org/10.1016/j.seta.2020.100895>.
 - [23] Mohamed MA, Jin T, Su W. An effective stochastic framework for smart coordinated operation of wind park and energy storage unit. *Appl Energy* 2020; 272:115228. <https://doi.org/10.1016/j.apenergy.2020.115228>.
 - [24] Gong X, Dong F, Mohamed MA, Awwad EM, Abdullah HM, Ali ZM. Towards distributed based energy transaction in a clean smart island. *J Clean Prod* 2020; 273:122768. <https://doi.org/10.1016/j.jclepro.2020.122768>.
 - [25] Mohamed MA, Jin T, Su W. Multi-agent energy management of smart islands using primal-dual method of multipliers. *Energy* 2020;208:118306. <https://doi.org/10.1016/j.energy.2020.118306>.
 - [26] Ahmad I, Shahabuddin S, Malik H, Harjula E, Leppanen T, Loven L, et al. Machine Learning Meets Communication Networks: Current Trends and Future Challenges. *IEEE Access* 2020;8:223418–60. <https://doi.org/10.1109/ACCESS.2020.3041765>.
 - [27] Sodhro AH, Sangaiah AK, Sodhro GH, Sekhari A, Ouzrout Y, Pirbhulal S. Energy-Efficiency of Tools and Applications on Internet. In: Sangaiah AK, Zhang Z, Sheng M, editors. *Comput. Intell. Multimed. Big Data Cloud with Eng. Appl.*, Academic Press; 2018. p. 297–318. 10.1016/B978-0-12-813314-9.00014-1.
 - [28] Sodhro AH, Obaidat MS, Pirbhulal S, Sodhro GH, Zahid N, Rawat A. A novel energy optimization approach for artificial intelligence-enabled massive internet of things. *Proc. 2019 Int. Symp. Perform. Eval. Comput. Telecommun. Syst. SPECTS 2019 - Part SummerSim 2019 Multiconference, Institute of Electrical and Electronics Engineers Inc.*; 2019. 10.23919/SPECTS.2019.8823317.
 - [29] Memon SK, Nisar K, Hijazi MHA, Chowdhry BS, Sodhro AH, Pirbhulal S, et al. A survey on 802.11 MAC industrial standards, architecture, security & supporting emergency traffic: Future directions. *J Ind Inf Integr* 2021;24:100225. 10.1016/J. JII.2021.100225.
 - [30] Sreeraj ES, Chatterjee K, Bandyopadhyay S. Design of isolated renewable hybrid power systems. *Sol Energy* 2010;84:1124–36. <https://doi.org/10.1016/j.solener.2010.03.017>.
 - [31] Kiwan S, Al-Nimr M, Salim I. A hybrid solar chimney/photovoltaic thermal system for direct electric power production and water distillation. *Sustain Energy Technol Assessments* 2020;38:100680. <https://doi.org/10.1016/j.seta.2020.100680>.
 - [32] Dursun E, Acarkan B, Kilic O. Modeling of hydrogen production with a stand-alone renewable hybrid power system. *Int J Hydrogen Energy* 2011;37: 3098–107. <https://doi.org/10.1016/j.ijhydene.2011.11.029>.
 - [33] Rohani G, Nour M. Techno-economical analysis of stand-alone hybrid renewable power system for Ras Musheib in United Arab Emirates. *Energy* 2014;64:828–41. <https://doi.org/10.1016/j.energy.2013.10.065>.
 - [34] Forough AB, Roshandel R. Multi objective receding horizon optimization for optimal scheduling of hybrid renewable energy system. *Energy Build* 2017. <https://doi.org/10.1016/j.enbuild.2017.06.031>.
 - [35] Harajli H, Kabakian V, El-Baba J, Diab A, Nassab C. Commercial-scale hybrid solar photovoltaic – diesel systems in select Arab countries with weak grids: An integrated appraisal. *Energy Policy* 2020;137:111190. <https://doi.org/10.1016/j.enpol.2019.111190>.
 - [36] Eltamaly AM, Addoweesh KE, Bawah U, Mohamed MA. New software for hybrid renewable energy assessment for ten locations in Saudi Arabia. *J Renew Sustain Energy* 2013;5:033126. <https://doi.org/10.1063/1.4809791>.
 - [37] Eltamaly AM, Addoweesh KE, Bawa U, Mohamed MA. Economic modeling of hybrid renewable energy system: a case study in Saudi Arabia. *Arab J Sci Eng* 2014;39:3827–39. <https://doi.org/10.1007/s13369-014-0945-6>.
 - [38] Eltamaly AM, Mohamed MA. A novel design and optimization software for autonomous PV/wind/battery hybrid power systems. *Math Probl Eng* 2014;2014. <https://doi.org/10.1155/2014/637174>.
 - [39] Suresh V, Muralidhar M, Kiranmayi R. Modelling and optimization of an off-grid hybrid renewable energy system for electrification in a rural areas. *Energy Rep* 2020. <https://doi.org/10.1016/j.egyr.2020.01.013>.
 - [40] Mokhtara C, Negrou B, Bouferrouk A, Yao Y, Setton N, Ramadan M. Integrated supply-demand energy management for optimal design of off-grid hybrid renewable energy systems for residential electrification in arid climates. *Energy Convers Manag* 2020;221:113192. <https://doi.org/10.1016/j.enconman.2020.113192>.
 - [41] Patel SK, Singh D, Devnani GL, Sinha S, Singh D. Potable water production via desalination technique using solar still integrated with partial cooling coil condenser. *Sustain Energy Technol Assessments* 2021;43:100927. <https://doi.org/10.1016/j.seta.2020.100927>.
 - [42] Petanat A, Tayebi M, Mofid H. Water-energy-food security nexus based selection of energy recovery from wastewater treatment technologies: An extended decision making framework under intuitionistic fuzzy environment. *Sustain Energy Technol Assessments* 2021;43:100937. <https://doi.org/10.1016/j.seta.2020.100937>.
 - [43] Ramesh M, Saini RP. Dispatch strategies based performance analysis of a hybrid renewable energy system for a remote rural area in India. *J Clean Prod* 2020;259: 120697. <https://doi.org/10.1016/j.jclepro.2020.120697>.
 - [44] Soberanis MAE, Mithruth T, Bassam A. A sensitivity analysis to determine technical and economic feasibility of energy storage systems implementation : A flow battery case study. *Renew. Energy* 2018;115. <https://doi.org/10.1016/j.renene.2017.08.082>.
 - [45] Sarker S. Feasibility analysis of a renewable hybrid energy system with producer gas generator full filling remote household electricity demand in Southern Norway. *Renew Energy* 2016;87:772–81. <https://doi.org/10.1016/j.renene.2015.11.013>.
 - [46] Shezan SKA, Julai S, Kibria MA, Ullah KR, Saidur R, Chong WT, et al. Performance Analysis of an off-grid Wind-PV-Diesel-Battery Hybrid Energy System Feasible for Remote Areas. *J Clean Prod* 2016. <https://doi.org/10.1016/j.jclepro.2016.03.014>.
 - [47] Upadhyay S, Sharma MP. Selection of a suitable energy management strategy for a hybrid energy system in a remote rural area of India. *Energy* 2016;94:352–66. <https://doi.org/10.1016/j.energy.2015.10.134>.
 - [48] Mexico Agenda 2030. Gov Mex Agenda 2030 2021. <https://www.gob.mx/agenda2030> (accessed January 30, 2021).
 - [49] Yucatan Agenda 2030. Gov Yucatan, Agenda 2030 2021. <http://www.seplan.yucatan.gob.mx/agenda2030/> (accessed January 30, 2021).
 - [50] Gude VG. Energy and water autarky of wastewater treatment and power generation systems. *Renew Sustain Energy Rev* 2015;45:52–68. <https://doi.org/10.1016/j.rser.2015.01.055>.
 - [51] Raheem A, Sikarwar VS, He J, Dastyar W, Dionysiou DD, Wang W, et al. Opportunities and challenges in sustainable treatment and resource reuse of sewage sludge: a review. *Chem Eng J* 2018;337:616–41.
 - [52] INEGI C de P. vivienda, Instituto Nacional de Geografía y Estadística 2014.
 - [53] Gobierno del Estado de Yucatán. San José Tip – Ceh 2020.
 - [54] JAPAY. Consumo de agua potable. (In Spanish) Los Desafíos Del Agua Http:// JapayYucatanGobMx/Noticias/VerarticuloPhp?IdArticulo=358 2019.
 - [55] Mara DD, Guimarães ASP. Simplified sewerage: Potential applicability in industrialized countries. *Urban Water* 1999;1:257–9. [https://doi.org/10.1016/s1462-0758\(99\)00015-1](https://doi.org/10.1016/s1462-0758(99)00015-1).

- [56] Tchobanoglous G, Burton F, Stensel HD. Wastewater engineering: Treatment and reuse. *Am Water Work Assoc J* 2003;95:201.
- [57] Velitchko GT, Víctor HA-Y. Modelación de la variación del consumo de agua potable con métodos estocásticos. *Tecnol Cienc Agua* 2016;7.
- [58] HYUNDAI. [In Spanish] Generador Hyundai Portatil 5.0-5.5 KW C/MOTOR 13 HP - HHY5500. Hyundai Power Prod 2021. <https://www.hyundaipower.com.mx/producto/generador-hyundai-portatil-5-0-5-5-kw-c-motor-13-hp-hhy5500/> (accessed May 9, 2021).
- [59] Tariq R, Xamán J, Bassam A, Ricalde LJ, Soberanis MAE. Multidimensional assessment of a photovoltaic air collector integrated phase changing material considering Mexican Climatic conditions. *Energy* 2020;209:118304. <https://doi.org/10.1016/j.energy.2020.118304>.
- [60] Messenger RA, Abtahi A. Photovoltaic systems engineering. CRC Press; 2017.
- [61] Sharp Solar. Módulo Fotovoltaico de Silicio Monocristalino NU-JB395L (144 células) 2020.
- [62] Kosmadakis IE, Elmasides C, Eleftheriou D, Tsagarakis KP. A techno-economic analysis of a PV-battery system in Greece. *Energies* 2019. <https://doi.org/10.3390/en12071357>.
- [63] enair. E200L Ficha Técnica. 2021.
- [64] Mongird K, Viswanathan V, Balducci P, Alam J, Fotedar V, Koritarov V, et al. Energy Storage Technology and Cost Characterization Report. 2019.
- [65] NREL. Distributed Generation Renewable Energy Estimate of Costs 2016.
- [66] Mohamed MA, Eltamaly AM. Sizing and Techno-Economic Analysis of Stand-Alone Hybrid Photovoltaic/Wind/Diesel/Battery Energy Systems. *Model. Simul. Smart Grid Integr. with Hybrid Renew. Energy Syst.*, Springer; 2018, p. 23–38.
- [67] Homer Energy. Homer Pro. Man Homer Energy 2019:1–241.
- [68] Bruck M. A Levelized Cost of Energy (LCOE) model for wind farms that includes Power Purchase Agreement (PPA) energy delivery limits availability-based real options approach for determining cost and pricing of performance-based logistics contracts view project. *Renew Energy* 2016;122:131–9.
- [69] Elevation Angle, PVEducation 2021. <https://www.pveducation.org/pvcdrom/properties-of-sunlight/elevation-angle> (accessed May 8, 2021).
- [70] Park CY, Hong SH, Lim SC, Song BS, Park SW, Huh JH, et al. Inverter efficiency analysis model based on solar power estimation using solar radiation. *Processes* 2020;8:1–19. <https://doi.org/10.3390/pr8101225>.
- [71] Rehman S, Al-Abbadi NM. Wind shear coefficients and their effect on energy production. *Energy Convers Manag* 2005;46:2578–91. <https://doi.org/10.1016/j.enconman.2004.12.005>.
- [72] May Tzuc O, Bassam A, Ricalde LJ, Jaramillo OA, Flota-Bañuelos M, Escalante Soberanis MA. Environmental-economic optimization for implementation of parabolic collectors in the industrial process heat generation: Case study of Mexico. *J Clean Prod* 2020;242:118538. <https://doi.org/10.1016/j.jclepro.2019.118538>.
- [73] [In Spanish] Índice Nacional de Precios al Consumidor (INPC), Instituto Nacional de Estadística y Geografía (INEGI) 2021. <https://www.inegi.org.mx/temas/inpc/> (accessed May 9, 2021).
- [74] NASA. NASA POWER Data Access Viewer 2021. <https://power.larc.nasa.gov/data-access-viewer/> (accessed May 8, 2021).
- [75] CFE (Comisión Federal de Electricidad). Consulta tu tarifa. 2017 2018. <https://app.cfe.mx/Aplicaciones/CCFE/Tarifas/TarifasCRECasa/Casa.aspx>.
- [76] Halabi LM, Mekhilef S, Olatomiwa L, Hazelton J. Performance analysis of hybrid PV/diesel/battery system using HOMER: A case study Sabah. Malaysia. *Energy Convers Manag* 2017;144:322–39. <https://doi.org/10.1016/j.enconman.2017.04.070>.
- [77] Alshammari N, Asumadu J. Optimum unit sizing of hybrid renewable energy system utilizing harmony search, Jaya and particle swarm optimization algorithms. *Sustain Cities Soc* 2020;60:102255. <https://doi.org/10.1016/j.scs.2020.102255>.
- [78] Homer Energy. HOMER – Hybrid Renewable and Distributed Generation System Design Software. <http://www.HomerEnergy.com> 2016.
- [79] Tariq R, Jimenez JT, Sheikh NA, Khan S. Mathematical approach to improve the thermoeconomics of a humidification dehumidification solar desalination system. *Mathematics* 2021;9:1–31. <https://doi.org/10.3390/math9010033>.
- [80] Caliskan H. Novel approaches to exergy and economy based enhanced environmental analyses for energy systems. *Energy Convers Manag* 2015;89:156–61. <https://doi.org/10.1016/j.enconman.2014.09.067>.
- [81] Sovacool BK. Valuing the greenhouse gas emissions from nuclear power: a critical survey. *Energy Policy* 2008;36:2950–63. <https://doi.org/10.1016/j.enpol.2008.04.017>.
- [82] Dai Q, Kelly JC, Gaines L, Wang M. Life cycle analysis of lithium-ion batteries for automotive applications. *Batteries* 2019;5:48. <https://doi.org/10.3390/batteries5020048>.
- [83] Gaines L, Sullivan J, Burnham A, Belharouak I. Life-cycle analysis of production and recycling of lithium ion batteries. *Transp Res Rec J Transp Res Board* 2011;2252:57–65. <https://doi.org/10.3141/2252-08>.
- [84] Peters JF, Baumann M, Zimmermann B, Braun J, Weil M. The environmental impact of Li-Ion batteries and the role of key parameters – a review. *Renew Sustain Energy Rev* 2017;67:491–506. <https://doi.org/10.1016/j.rser.2016.08.039>.
- [85] Hawkins TR, Singh B, Majeau-Bettez G, Strømman AH. Comparative environmental life cycle assessment of conventional and electric vehicles. *J Ind Ecol* 2013;17:53–64. <https://doi.org/10.1111/j.1530-9290.2012.00532.x>.
- [86] Hu A, Huang L, Lou S, Kuo C-H, Huang C-Y, Chian K-J, et al. Assessment of the carbon footprint, social benefit of carbon reduction, and energy payback time of a high-concentration photovoltaic system. *Sustainability* 2016;9:27. <https://doi.org/10.3390/su9010027>.
- [87] Kawamoto R, Mochizuki H, Moriguchi Y, Nakano T, Motohashi M, Sakai Y, et al. Estimation of CO2 emissions of internal combustion engine vehicle and battery electric vehicle using LCA. *Sustainability* 2019;11:2690. <https://doi.org/10.3390/su11092690>.
- [88] Tariq R, Sohani A, Xamán J, Sayyaadi H, Bassam A, Tzuc OM. Multi-objective optimization for the best possible thermal, electrical and overall energy performance of a novel perforated-type regenerative evaporative humidifier. *Energy Convers Manag* 2019;198:111802. <https://doi.org/10.1016/j.enconman.2019.111802>.
- [89] Golizadeh Akhlaghi Y, Badieli A, Zhao X, Aslansefat K, Xiao X, Shittu S, et al. A constraint multi-objective evolutionary optimization of a state-of-the-art dew point cooler using digital twins. *Energy Convers Manag* 2020. <https://doi.org/10.1016/j.enconman.2020.112772>.
- [90] MathWorks. The Language of Technical Computing 2017. <https://www.mathworks.com/products/matlab.html>.
- [91] Sohani A, Sayyaadi H, Hoseinpoori S. Modeling and multi-objective optimization of an M-cycle cross-flow indirect evaporative cooler using the GMDH type neural network Modélisation et optimisation à objectifs multiples d'un refroidisseur évaporatif indirect à écoulements croisés à cycle M e. *Int J Refrig* 2016;69:186–204. <https://doi.org/10.1016/j.ijrefrig.2016.05.011>.
- [92] Tariq R, Hussain Y, Sheikh NA, Afaq K, Ali HM. Regression-Based Empirical Modeling of Thermal Conductivity of CuO-Water Nanofluid using Data-Driven Techniques. *Int J Thermophys* 2020;41. <https://doi.org/10.1007/s10765-020-2619-9>.
- [93] Sohani A, Sayyaadi H. Design and retrofit optimization of the cellulose evaporative cooling pad systems at diverse climatic conditions. *Appl Therm Eng* 2017;123:1396–418. <https://doi.org/10.1016/j.applthermaleng.2017.05.120>.
- [94] Jamil MA, Goraya TS, Shahzad MW, Zubair SM. Exergoeconomic optimization of a shell-and-tube heat exchanger. *Energy Convers Manag* 2020;226:113462. <https://doi.org/10.1016/j.enconman.2020.113462>.
- [95] STATGRAPHICS Centurion 2021. <https://www.statgraphics.com/> (accessed May 11, 2021).
- [96] Kim JH, Simon TW. Journal of heat transfer policy on reporting uncertainties in experimental measurements and results. *J Heat Transfer* 1993;115:5–6. <https://doi.org/10.1115/1.2910670>.
- [97] Hussaini IS, Zubair SM, Antar MA. Area allocation in multi-zone feedwater heaters. *Energy Convers Manag* 2007;48:568–75. <https://doi.org/10.1016/j.enconman.2006.06.003>.
- [98] Qureshi BA, Zubair SM. A comprehensive design and rating study of evaporative coolers and condensers. Part II. Sensitivity analysis. *Int J Refrig* 2006;29:659–68. <https://doi.org/10.1016/j.ijrefrig.2005.09.015>.
- [99] Jamil MA, Ud Din Z, Goraya TS, Yaqoob H, Zubair SM. Thermal-hydraulic characteristics of gasketed plate heat exchangers as a preheater for thermal desalination systems. *Energy Convers Manag* 2020;205:112425. <https://doi.org/10.1016/j.enconman.2019.112425>.
- [100] James CA, Taylor RP, Hodge BK. The application of uncertainty analysis to cross-flow heat exchanger performance predictions. *Heat Transf Eng* 1995;16:50–62. <https://doi.org/10.1080/01457639508939863>.
- [101] Software F-Chart. EES: Engineering Equation Solver: Engineering Software. F-Chart Softw 2015;2012:6–8. <http://www.fchart.com/ees/> (accessed September 28, 2018).
- [102] CFE. Tarifas-GranDemandaMTO 2021.
- [103] Shahzad M, Ma T, Jurasz J, Canales FA, Lin S, Ahmed S, et al. Economic analysis and optimization of a renewable energy based power supply system with different energy storages for a remote island. *Renew Energy* 2020;164:1376–94. <https://doi.org/10.1016/j.renene.2020.10.063>.
- [104] Ramli MAM, Bouchekara HREH, Alghamdi AS. Optimal Sizing of PV/wind/diesel hybrid microgrid system using multi-objective self-adaptive differential evolution algorithm. *Renew Energy* 2018. <https://doi.org/10.1016/j.renene.2018.01.058>.
- [105] Usman M, Khan MT, Rana AS, Ali S. Techno-economic analysis of hybrid solar-diesel-grid connected power generation system. *J Electr Syst Inf Technol* 2018;5:653–62. <https://doi.org/10.1016/j.jesit.2017.06.002>.
- [106] Rajanna S, Saini RP. Development of optimal integrated renewable energy model with battery storage for a remote Indian area. *Energy* 2016;111:803–17. <https://doi.org/10.1016/j.energy.2016.06.005>.
- [107] El Mekaoui A, Tariq R, Ramírez OB, Méndez-Monroy PE. Sustainability, sociocultural challenges, and new power of capitalism for renewable energy megaprojects in an indigenous Mayan Community of Mexico. *Sustain* 2020;12:7432. <https://doi.org/10.3390/SU12187432>.
- [108] Objective Scatter Index. Indian Natl Cent Ocean Inf Serv 2021.
- [109] Golbraikh A, Tropsha A. Beware of q²! *J Mol Graph Model* 2002;20:269–76. [https://doi.org/10.1016/S1093-3263\(01\)00123-1](https://doi.org/10.1016/S1093-3263(01)00123-1).